AIAA-91-1207-CP

# OPTIMIZATION OF A TEE-STIFFENED PANEL UNDER AXIAL COMPRESSION, IN-PLANE SHEAR, AND NORMAL PRESSURE

David Bushnell

Consulting Scientist, Lockheed Palo Alto Research Laboratory
Dept. 93-30, Bldg. 251, 3251 Hanover St., Palo Alto, CA 94304

## ABSTRACT

The PANDA2 computer program is used to find a minimum weight design of a flat panel with T-shaped stringers. The panel is allowed to buckle locally under the specified loading. The evolution of the design is influenced by stress and buckling constraint conditions at the midlength and at the ends of the panel. These constraint conditions are very different because bending of the panel under the pressure gives rise to very different distributions of stress over the cross section of skin and stringers which cause different buckling and postbuckling behaviors at these locations.

## INTRODUCTION

There is an extensive literature on the buckling and postbuckling behavior of stiffened plates and shells. This literature covers metallic panels and panels fabricated from laminated composite materials. Leissa [1] has gathered results from almost 400 sources on the buckling and postbuckling behavior of flat and cylindrical panels made of composite material with various stacking sequences and boundary conditions and subjected to various in-plane loads. The emphasis in his survey is on theoretical results, although some experimental results are included. He includes several examples in which the effect of transverse shear deformation is explored. Emphasis is given also to the effects of anisotropy on bifurcation buckling and on postbuckling behavior. Wiggenraad [2] surveys the literature on design of composite panels permitted to buckle locally under operating loads. Included in his survey are damage tolerance, fatigue, and optimization. Arnold and Parekh [3] emphasize in their survey and theoretical development the effect of in-plane shear load on the postbuckling behavior of stiffened, composite cylindrical panels. Surveys of earlier work on buckling of stiffened panels and shells appear in [4] and [5].

Among the foremost contributors of information about buckling of stiffened shells are Josef Singer and his colleagues at the Technion in Haifa, Israel. In particular, the Baruch-Singer theory [6] for averaging the properties of stiffeners over a shell surface while retaining the important eccentricity effects has been incorporated into many widely used computer programs for the stress, vibration, and buckling analysis of stiffened shells.



The literature in the field of buckling of stiffened shells can be divided into three categories, one in which test results are emphasized, a second in which structural analysis is emphasized, and a third in which optimum designs are obtained. References [7] through [17] feature test results for plates, shells, and stiffeners made of laminated composite material; [18] through [25] feature structural analysis with structural properties fixed; and [26] through [35] feature structural analysis with optimum configurations sought in most cases via the widely used optimizers CONMIN and ADS, written by Vanderplaats and his colleagues [36 - 38]. This is just a sample of the literature on the subject. The reader is referred to the surveys given in [1] through [5] and references cited there for other sources.

## PURPOSES OF THIS PAPER

The purposes of this paper are to reveal the interesting buckling and postbuckling behavior of a stiffened panel under combined axial compression, in-plane shear, and normal pressure, and to demonstrate how a preliminary optimum design of such a panel can be obtained in the presence of the extremely nonlinear behavior associated with local buckling and postbuckling. Although the example presented here involves only isotropic material, the PANDA2 program was created with laminated composite wall construction in mind. The material is assumed to be elastic, although its properties can be temperature-dependent.

Details about PANDA2 and the theory on which it is based appear in [35,41,42]. Therefore only a summary of its scope is provided here.

## REVIEW OF THE SCOPE AND PHILOSOPHY OF PANDA2

The purpose of PANDA2 is to find the minimum weight design of a stiffened flat or curved, perfect or imperfect, panel made of laminated composite material.

### Geometry

The kinds of stiffening handled by PANDA2 are:

1. unstiffened
2. T-shaped stiffeners
3. J-shaped stiffeners
4. Rectangular (blade) stiffeners
5. Hat-shaped stiffeners
6. truss-core sandwich (with no other stiffeners)

The properties of the panel are assumed to be uniform in the axial (x) direction and periodic (consisting of repetitive modules) in the circumferential (y) direction. If the panel is other than of truss-core sandwich construction, it may be stiffened by uniformly spaced stringers alone, stiffened by uniformly spaced rings alone, or stiffened by both rings and stringers. All stringers must be the same. All rings must be the same. The rings can be different from the stringers. Truss-core sandwich panels cannot be further stiffened by either stringers or rings.

Note that the theory on which PANDA2 is based is valid only if the panel is either unstiffened or, if stiffeners exist in either or both coordinate directions, there are several of them within the span of the panel. One cannot accurately determine the behavior of a panel with only one stiffener, for example. The panel, if axially stiffened, for example, has a "field" of equally spaced, identical stringers.

In PANDA2 local buckling behavior is predicted from analysis of a single module which is assumed to repeat several times over the width of the panel, as shown in Fig. 1.

A panel module consists of one stiffener plus skin of width equal to the spacing between stiffeners (Fig. 2). The single module is considered to be composed of segments, each of which has its own laminated wall construction (Fig. 3).

General instability is predicted from a model in which the stiffeners are "smeared" in the manner of Baruch and Singer [6] over the width (stringers) and length (rings) of the panel.

## Boundary Conditions

In the PANDA2 system the panel is assumed to be simply supported along the two edges normal to the plane of the screen (at y = 0 and at y = panel width). The panel can be either simply supported or clamped along the other two boundaries (at x = 0 and x = L), but the conditions must be the same at both of these two boundaries. The PANDA2 analysis is always performed for simple support on all four edges. However, experience has shown that for the purpose of calculating panel and general instability load factors, clamping at x = 0 and at x = L can be simulated by the analysis of a shorter simply supported panel: For example, an axially compressed, flat panel clamped at x = 0 and x = L has general instability loads approximately equal to those of a panel simply supported at x = 0 and x = L/sqrt{3.85}. In PANDA2, clamping at x = 0 and x = L is simulated by calculation of general instability or wide column instability of a simply supported panel with a shorter length, an "effective" length that depends on the ratios of in-plane loads and on the "boundary layer length" in the axial direction. This "effective" length is calculated by PANDA2 and is provided as output.

In PANDA2 local buckling behavior and local stress concentrations near stringers are assumed to be independent of the boundary conditions along the four panel edges. This is likely to be a good assumption if there are more than two or three halfwaves in the local buckling pattern over the length and width of the panel.

## Loading

PANDA2 allows the panel to be loaded by as many as five independent sets of in-plane load combinations, Nx, Ny, Nxy, Mx, My, normal pressure p, and temperature T(z) that is nonuniform over the panel cross section but uniform in the (x,y) coordinates. Buckling loads, postbuckling behavior, and maximum stresses are calculated for each of the five load sets applied by itself. PANDA2 determines the best design that is capable of surviving all of the five load sets when each set is applied separately, as it would be during different phases of a panel's lifetime or over different areas of a large, uniform structure such as a complete cylindrical shell subjected to spatially varying loads (See [35]). Associated with each of the five independent load sets there can be two load subsets, Load Set A and Load Set B. Load Set A consists of what are termed in the PANDA2 output as "eigenvalue loads": These are loads that are to be multiplied by the critical buckling load factor (eigenvalue). Load Set B consists of loads that are not multiplied by the critical buckling load factor.

## Types of Analysis

PANDA2 performs the following analyses:

1. CONSTITUTIVE LAW:

a. PANDA2 computes the integrated constitutive law [the 6x6 matrix C(i,j) that relates reference surface strains, changes in curvature, and twist to stress and moment resultants] for each segment of a panel module.

b. It computes thermal resultants and strains from curing and from applied temperature during service for each segment of a panel module.

c. It computes the integrated constitutive law [the 6x6 matrix Cs(i,j)] for the panel with either and both sets of stiffeners "smeared out". ("Smearing out" the stiffeners means averaging their properties over the entire area of the panel as prescribed by Baruch and Singer [6]).

d. It computes the tangent stiffness CTAN(i,j) of the panel skin in its locally postbuckled state, if applicable.

e. It computes the tangent stiffness CsTAN(i,j) of the panel with smeared stiffeners, using CTAN(i,j) for the locally postbuckled stiffness of the panel skin.

2. EQUILIBRIUM:

a. PANDA2 computes bowing of the panel due to curing.

b. It computes static response of the panel to uniform normal pressure, using either linear or nonlinear theory. Two problems are solved:

b(1) overall static response of entire panel with smeared stiffeners, and

b(2) local static response of a single panel module with a discretized cross section.

c. Average strain and resultant distribution in all of the panel module cross section segments are determined for:

c(1) the panel loaded by all loads except normal pressure. The effect of bowing of the panel due to curing, applied temperature during service, normal pressure, and edge moments is included, as well as the effect of an initial imperfection in the form of axial bowing.

c(2) the panel loaded by normal pressure.

d. Stresses in material coordinates in each layer in each laminate (segment) of the panel module are calculated either for the post-locally buckled panel, or for the unbuckled panel, whichever is applicable. The effect of a local imperfection in the form of the local buckling mode is included, as well as axial bowing from either cure, temperature change during service, pressure, edge moments, eccentrically applied axial load, initial imperfection, or any combination of these effects.

e. Tensile forces in parts of the stiffener web(s) that tend to pull the web from the panel skin are calculated, and these forces are compared to a maximum allowable "peel force" that the user has previously obtained from peel tests on sample coupons that bear some similarity to the concept for which he or she is seeking an optimum design.

3. BUCKLING:

a. PANDA2 computes buckling load factors from a PANDA-type of analysis (closed form, see Ref [4]) for general instability, local buckling of the panel skin, local buckling of stiffener segments, and rolling of stiffeners with and without participation of the panel skin.

b. It computes the load factor for local skin buckling from a BOSOR4-type [39] of analysis (finite strip method) in which the cross section of a single panel module is discretized, as shown in Fig. 4 of this paper.

c. It computes a load factor for wide column buckling from a BOSOR4-type of analysis of a discretized single panel module. In this analysis the reduced effective stiffness of the locally buckled panel skin is used, if applicable.

d. If the axial load varies over the width of the panel, PANDA2 computes a load factor for general instability from a BOSOR4-type of analysis of the entire panel with smeared stiffeners. The width of the panel is discretized. Again, the reduced effective stiffness of the locally buckled panel skin is used for this analysis, if applicable.

e. PANDA2 generates a refined discretized model of the entire panel width with stringer parts treated as flexible shell branches. This model can be used directly as input to BOSOR4.

Philosophy embodied in PANDA2

PANDA2 represents a more detailed treatment of certain behavior not handled by PANDA [4]. In particular, optimum designs can be obtained for imperfect panels, for panels with locally post-buckled skin for panels with hat stiffeners, and for panels with truss-core sandwich construction. In addition, PANDA2 will handle linear or nonlinear static response to normal pressure, panels with nonuniform axial loading, panels with edge moments, and panels with thermal loading and temperature-dependent material properties. Also, PANDA2 optimizes panels for multiple sets of loads, whereas PANDA [4] optimizes for a single set of in-plane loads.

Optimization is carried out based on several independently treated structural models of the panel. These might be classified into three model types, as follows:

1. Model type 1: Included are PANDA-type models [4] for general, local, and panel buckling, bifurcation buckling of stiffener parts, and rolling of stiffeners with and without participation of the panel skin. With PANDA-type models, buckling load factors are calculated from closed-form equations rather than from discretized models. The formulas are given in [4]. (See Table 1 and Figs. 1-4 of [4]).

2. Model type 2: Buckling load factors and post-local buckling behavior are calculated for what is termed in PANDA2 a "panel module." A module includes the cross section of a stiffener plus the panel skin of width equal to the spacing between stiffeners. In this model the panel module cross section is divided into segments, each of which is discretized and analyzed via the finite difference energy method [39] (finite strip method). Variation of deflection in the axial direction is assumed to be harmonic [sin(nx) or cos(nx)]. This one-dimensional discretization is similar to that used in the BOSOR programs for the analysis of shells of revolution [39]. In fact, many of the subroutines for buckling and vibration analysis are taken from BOSOR4 and modified slightly in order to handle prismatic structures instead of shells of revolution.

The single module model gives a good approximation to the local skin buckling mode if there are more than three equally spaced stringers in the panel. What goes on locally between interior stringers in a panel, stringers which are rotating about their axes only, not bending, is only weakly affected by the boundary conditions at panel edges that may be several bays away.

Both local and wide-column instability can be handled with the same discretized structural model. For all except truss-core sandwich panels, symmetry conditions are applied at the left and right edges of the single module model, that is, symmetry conditions are applied midway between stringers. Edge conditions for the single module of the truss-core sandwich panel are discussed later.

The wide column buckling model in PANDA2 is applied to an axial length of panel between adjacent rings, or if there are no rings, to the entire axial length of the panel, L or for clamped panels the modified length L/sqrt{3.85}. The wide-column buckling load predicted from the single panel module is always lower and, if the panel is not of the truss-core sandwich type and is stringer-stiffened, usually reasonably close to the general instability load of the entire width of the panel between rings because the axial bending stiffness of a stringer-stiffened panel is usually much, much greater than the transverse bending stiffness of the portion of the panel between adjacent rings. Hence, the strain energy in the buckled panel, and therefore the buckling behavior, is only weakly dependent on bending of the panel transverse to the stringers. Therefore, the boundary conditions along the edges of the panel parallel to the stringers are not important. On the other hand, local bending of the skin and local deformation of the stringer parts in the wide column buckling mode may significantly affect the wide column buckling load. These effects are not included in the closed-form PANDA-type model of general instability, but they are included in the single panel module model of wide column buckling.

The wide-column buckling model should not be used for prediction of general buckling of truss-core sandwich panels. It is too conservative because, unlike T, J, Blade, and Hat-stiffened panels, sandwich panels have bending stiffnesses in the x and y directions which are of the same magnitude. Therefore, one cannot ignore the longitudinal boundaries in the calculation of general instability load factors of truss-core sandwich panels.

3. Model type 3: Also included in the PANDA2 collection of models is a discretized model of the entire width of the panel, treated in this case with stiffeners smeared out. This model is introduced only if the axial load varies across the width of the panel or if there exists normal pressure.

The purpose PANDA2 is to yield optimum PRELIMINARY designs of rather sophisticated panels that may experience very complex and very nonlinear behavior. The goal is to do this without having to use large, general-purpose programs with their elaborate data base management systems. This goal is achieved through the use of several separate relatively simple models, each designed to capture a specific phenomenon, rather than through the use of a single multi-dimensionally discretized finite element model with a large number of degrees of freedom.

For example, PANDA-type models (Model type 1) are used in PANDA2 to obtain quick, preliminary designs which one can then use as starting designs in optimization analyses based on the more elaborate discretized panel module model. Also, PANDA-type models are used to obtain buckling load factors in cases for which the discretized panel module model is not applicable, to obtain knockdown factors for the effect of in-plane shear loading, to obtain preliminary estimates of how much growth in any initial panel bowing to expect under compressive in-plane loads, and to check if it is likely that a curved panel with uniform external pressure will collapse under the pressure acting by itself.

Models of type 2 (single discretized module) and type 3 (discretization of entire width with smeared stiffeners) are used in tandem to obtain from nonlinear theory the complex behavior of a stiffened plate or shell loaded by normal pressure. Model type 3 is the only one that is valid if the axial load varies across the width of the panel.

In the panels designed by PANDA2 the skin between stringers and the stringer parts will deform if they are locally imperfect, and even if they are perfect they may buckle well before failure of the panel. The maximum stress components and therefore stress constraints in the optimization analysis are computed including local prebuckling deformation and local post buckling growth and modification of the local skin buckling mode as predicted by a modified form of a theory formulated by Koiter in 1946 [40, 35]. Model type 2 (single discretized module) is the only model in PANDA2 valid for these analyses.

After the optimum design is obtained, the user can, if no in-plane shear load is applied, check the accuracy of the general instability load predicted from the single-module model by running a multi-module model with BOSOR4 [39]. The input data file for this multi-module model is generated automatically by the PANDA2 system.

## Architecture of the PANDA2 system

As with PANDA [4], the program PANDA2 [35] consists of several independently executable processors which share a common

data base. In the processor BEGIN the user supplies a starting design (perhaps a design produced by PANDA). In DECIDE the user chooses decision variables for the optimization analysis and their upper and lower bounds, linking variables and their factors of proportionality, and "escape" variables (explained in [35]). In MAINSETUP the user chooses up to five sets of combined in-plane loads and normal pressure; factors of safety for general instability, panel (between rings) instability, local instability, and material failure; strategy parameters such as number and range of axial half-waves in the local buckling mode; and number of design iterations in the optimization problem. The command PANDAOPT initiates a batch run of the PANDA2 mainprocessor, which consists of two main branches: in one branch the structural analyses (stress, buckling and post-buckling) are performed and in the other new designs are produced by the optimizer ADS [37, 38].

Improvements to PANDA2

1. Plots of dimensions, objective, and design margins vs. design iterations are generated by new processors, CHOOSEPLOT and DIPLOT, described in [41]. The plots in [42] and here were generated with the CHOOSEPLOT/DIPLOT processors.

2. There is new flexibility with regard to the in-plane movability of the edges as the panel is loaded by normal pressure. Indeed, with movable boundaries of flat panels especially, the increased bowing and lack of development of average in-plane tension caused by bending can greatly reduce local buckling load factors, affecting the local postbuckling behavior and therefore the stress constraints that influence the evolution of the optimum design during optimization iterations.

3. New logic has been introduced to generate a "knockdown" factor to compensate for the inherent unconservativeness of smearing stiffeners in the prediction of general (overall) and panel (between rings) instability, especially in cases where there is significant applied in-plane shear loading. The amount of knockdown is related to the ratio of the wavelength of the buckles in the in-plane coordinate y normal to the stiffeners to the spacing b of the stiffeners.

4. Edge moments may be applied to the panel.

5. Temperature distributions may be applied to the panel and the material may be temperature-dependent. (Material must still behave linearly, however).

6. If the panel is loaded by normal pressure, buckling and stress constraints are generated for conditions both at the midlength and at the ends of the panel. This modification is important because the very different distributions of axial compression over the skin-stringer cross section cause very different buckling and stress behavior at these different axial locations. Behavioral constraint conditions corresponding to both panel midlength and panel ends may influence the evolution of the design during optimization iterations.

7. A new behavioral constraint condition based on bending-torsional buckling with a long axial wavelength has been introduced.

8. There may now be different boundary conditions for the prebuckling and bifurcation buckling phases of the problem. This modification is important for finding optimum designs of panels under normal pressure in which the panel being optimized spans large rings. In the prebuckling phase the rings act like clamps, preventing edge rotation because of symmetrical behavior on either side of the ring. However, practical rings, especially those with open cross sections, are likely to be too weak to prevent edge rotation in the bifurcation buckling phase of behavior. Therefore, simple support conditions are usually called for then.

9. If the panel is considered to be clamped in the prebuckling phase and if it is axially stiffened, its overall response to normal pressure is predicted from simple wide-beam bending theory. The theory is taken from Roark [43]. At the midlength of the panel the change in curvature is given by:

$$\text{Kappa}(x) = (1/24)*p*L**2/C44(\text{neutral axis}) \quad (1)$$

and the amplitude of the normal deflection is given by:

$$\text{Wpressure} = (1/384)*p*L**4/C44(\text{neutral axis}) \quad (2)$$

At the ends of the panel the change in curvature is given by:

$$\text{Kappa}(x) = -(1/12)*p*L**2/C44(\text{neutral axis}) \quad (3)$$

and the maximum web shear resultant, Nxy(due to pressure) is

$$Nxy(p) = (1/2)*p*L*b/h \quad (4)$$

In the formulas above, p is the normal pressure, positive as shown in Fig. 8, page 490 of [35], L is the length of the panel between the large rings (which are not present as actual structures in the PANDA2 model, and C44(neutral axis) is the bending stiffness per transverse arc length when the reference surface is the neutral plane in the x-direction.

The beam bending model is used only for the deformation of the entire panel with smeared stiffeners. The local model for bending and stretching under pressure (single module) has not been changed, except that the user now has a choice as to whether the longitudinal edges are in-plane movable or not.

10. More general linking expressions and inequality constraints based on the panel cross section dimensions have been introduced into the DECIDE processor. A general expression for a linked variable now has the form:

```
(linked variable)  =
      C1*(decision variable no. j1)
     +C2*(decision variable no. j2)
     +C3*(decision variable no. j3)
     +etc (up to max. of 5 terms)
     +C0                                    (5)
```

in which C1, C2,..; and C0 are constants. Inequality relations among variables may have either of the two forms:

```
       1.0 < f(v1,v2,v3,...)
  or   1.0 > f(v1,v2,v3,...)                (6)
```

where the expression f(v1,v2,v3,...) has the form:

```
f(v1,v2,v3,...) =
    C0 +C1*v1**D1 +C2*v2**D2 +C3*v3**D3
    + ... +etc (up to max. of 5 terms).  (7)
```

The variables, v1, v2, v3,..., can be any of the variables that are decision variables or potential candidates for decision variables or linked variables.

11. Whereas formerly there were two choices for type of analysis,

(1) optimization and
(2) analysis of a fixed design at a fixed load,

there is now a third choice:

(3) test simulation.

In this mode the user supplies starting loads, load increments and the number of load steps. PANDA2 calculates the response of a panel of fixed design for a number of load steps until general instability is detected or until the maximum number of load steps specified by the user is reached.

12. The assumed displacement field for calculation of PANDA-type buckling load factors has been modified for flat panels. In [4b] a Rayleigh-Ritz method for obtaining bifurcation buckling loads of anisotropic flat and cylindrical panels is described. The assumed displacement field (u,v,w) for the buckling mode is given by Eqs. (50), p 552, of [4b]:

```
u = A[n2**2*m1*sin(n1*y-m1*x)
     +n1**2*m2*sin(n2*y+m2*x)]

v = B[      n2*sin(n1*y-m1*x)
           -n1*sin(n2*y+m2*x)]                (8)

w = C[         cos(n1*y-m1*x)
              -cos(n2*y +m2*x)]
```

in which n1, n2, m1, m2 are given by

```
    n1 = n+mc;    n2 = n-mc;
    m1 = m+nd;    m2 = m-nd                  (9)
```

where c and d are the slopes of the buckling nodal lines as shown in Fig. 9 of [4b]. The axial and circumferential wave indices m and n are defined as

```
m = M*pi/x(max);     n = N*pi/y(max)        (10)
```

where M and N are the number of halfwaves over the axial length x(max) and the circumferential length y(max), respectively.

This formulation has been retained because it usually gives the best results for curved (cylindrical) panels, especially if the curved panel spans more than one radian. However, while comparing buckling loads for flat panels with unbalanced laminates from results obtained with the STAGS computer program [21,22], especially when in-plane shear predominates, it was found that the following assumed displacement pattern yields better predictions:

```
u = A[m1*sin(n1*y-m1*x)
    + m2*sin(n2*y+m2*x)]

v = B[n1*sin(n1*y-m1*x)
    - n2*sin(n2*y+m2*x)]                    (11)

w = C[   cos(n1*y-m1*x)
        -cos(n2*y+m2*x)]
```

13. A rather elaborate strategy has been introduced to obtain improved accuracy of buckling load factors for curved panels in which in-plane shear is a significant load component. Details of the strategy are included in the file called "PANDA2.NEWS", which forms part of the PANDA2 literature distributed with the program.

14. The local postbuckling theory, based on the work of Koiter [40], has been improved to allow for change in the axial wavelength of the local buckles as the panel is loaded further and further into the postbuckling regime.

15. Axial bending induced by neutral plane shift after local buckling has been introduced into the local postbuckling anslysis.

16. The PANDA2 user may now obtain plots of extreme fiber strains vs. load (test simulation mode) at several user-selected points in the panel module cross section.

17. The move limits for decision variables during optimization cycles now depend to a certain extent on the value of the gradients of the behavioral constraint conditions.

18. The thermal buckling capability of PANDA2 has been improved. It is now possible to perform an ITYPE=3 analysis (test simulation) with thermal loading only.

19. PANDA2 now runs with UNIX-based operating systems.

## NUMERICAL RESULTS FOR A TEE-STIFFENED PANEL WITH AXIAL COMPRESSION, Nx, IN-PLANE SHEAR, Nxy, AND NORMAL PRESSURE, p

### Configuration and loading

Figure 4 shows the geometry and loading. During optimization the axial load Nx = -500 lb/in, the in-plane shear load Nxy = + 500 lb/in, and the normal pressure p = 5.0 psi. The panel is 30 inches long and 24 inches wide. The pressure acts so as to bend the panel upward, as shown in the insert at the bottom left of Fig. 4. At the panel midlength, therefore, the skin is compressed more than the stringers, whereas the opposite is true at the panel ends. As mentioned in Item 6 above, conditions at both the midlength and at the panel ends are considered during optimization.

There is a single load set, but two subcases:

1. Subcase 1 corresponds to conditions at the panel midlength;

2. Subcase 2 corresponds to conditions at the panel ends.

The panel is considered to be clamped at the axially loaded ends in both the prebuckling and bifurcation buckling phases of the problem. Symmetry conditions apply along the other two edges.

Decision variables are variables that are permitted to change during optimization iterations. Possible decision variables in this example are identified in the upper left-hand portion of Fig. 4. They represent all of the dimensions of the skin-stringer panel module cross section. The material is isotropic and elastic.

The user-selected name for the case is TEE. The input data for the BEGIN processor (in which the user supplies the starting dimensions, material properties, boundary conditions) are listed in Table 1.

Results for two cases are discussed below:

1. Stringer spacing fixed at 8.0 inches.

2. Stringer spacing allowed to vary during optimization.

### Optimization (Analysis type 1: ITYPE = 1) with stringer spacing b fixed at 8.0 inches

Figures 5 - 11 are plots of the objective (panel weight), design variables, and design margins v. optimization iterations for a case in which the stringer spacing b is held constant at 8.0 inches. These plots were generated by execution of CHOOSEPLOT/DIPLOT, two of the processors of the PANDA2 system. Several PANDAOPT runs were made with different settings of certain strategy parameters during the search for an optimum design. This case was run in the following way:

1. There were 4 sets of 5 iterations each with use of IQUICK = 1. Note that each set of 5 iterations generates six points in Fig. 5 because the current starting design (zeroth iteration) is plotted with each set. IQUICK=1 means that closed-form PANDA-type formulas [4,4b] are used for the buckling analysis, referred to as "Model type 1" in the "philosophy" section above. This is the "quick" mode, used for initial iterations when we are presumably far from an optimum design. The discretized single-module model (Fig. 3) is used for computation of the local response of the panel skin to the uniform normal pressure, as described on p 555 of [35]. No nonlinar postbuckling analysis is performed.

2. There were 2 sets of 5 iterations each with IQUICK = 0 and the factor of safety for local buckling, FSLOC = 1.0. IQUICK=0 means that buckling load factors are calculated both from the PANDA-type closed formulation (Model type 1) and from the discretized panel module models (Model type 2). Local postbuckling behavior is accounted for. However, with FSLOC = 1.0 the local buckling constraint condition prevents the generation of configurations in which there is much local deformation of the panel cross section under the applied load system. There is some local deformation because the panel has a small initial local imperfection in the form of the predicted local buckling mode, but not much because feasible designs have local buckling load factors that are greater than unity during these iterations.

3. During all the iterations so far, the factor of safety for local buckling, FSLOC, was equal to 1.0 (which PANDA2 resets to 1.1 if IQUICK = 0). Therefore, local buckling was not permitted during these iterations (iterations from 0 through 36 in Figs 5 - 11).

4. After the 6th execution of PANDAOPT the factor of safety for local buckling FSLOC was reduced to 0.1. This means that local buckling between stringers is permitted; local buckling load factors will no longer constrain the design unless the local buckling load is less than 10 percent of the user-specified applied load system, Nx, Nxy, p.

5. Runs 7 - 9 were made with maximum permitted number of design iterations set at 5.

6. Before Run 10 was launched the maximum permitted number of design iterations was set equal to 25. PANDA2 decided that convergence to an optimum design had been achieved after 21 iterations.

Figure 5 summarizes the description just given. Notice that if local buckling is permitted (factor of safety for local buckling, FSLOC is less than unity) the optimum design is about 37 per cent lighter than the optimum obtained when local buckling is not permitted. Note that the design is optimum for a stringer spacing b = 8.0 inches. As will be seen later, a

lighter design evolves when the stringer spacing b is allowed to vary during optimization cycles.

Figures 6 and 7 show the evolution of cross section widths and thicknesses, respectively. Figures 8 and 9 give the margins for buckling and stress, respectively, corresponding to conditions at the midlength of the panel (Subcase 1). Figures 10 and 11 give the same for conditions at the panel ends (Subcase 2).

The following observations pertain to conditions at the midlength of the panel (Figs. 8 and 9):

1. If local postbuckling is not permitted the only critical constraint on the design is local buckling. No general instability critical margins are generated for conditions at the panel midlength, where the skin is compressed more than the stringers.

2. If local postbuckling is permitted the only critical constraint on the design is maximum stress.

The following observations pertain to conditions at the ends of the panel (Figs. 10 and 11):

1. If local postbuckling is not permitted, buckling of the webs and flanges of the stringers (which are compressed much more than the skin at the panel ends because of bending induced by the normal pressure) is critical. If IQUICK = 0 wide column buckling becomes critical because there is significant local deformation of the stringer web and flange caused by growth of the assumed local imperfection just prior to bifurcation buckling. This local deformation leads to reduction of the effective axial stiffnesses of these stinger parts, reducing the load factor for overall buckling.

2. If local postbuckling is permitted there are no critical margins for conditions at the panel ends at the optimum design. However, several modes of failure (rolling of stringers, web buckling of stringers, flange buckling of stringers, wide column buckling, and maximum allowable effective stress at one tip of the stringer flange) have margins of about 20 percent.

3. The margins for maximum effective stress and wide column buckling may vary rather wildly from iteration to iteration, especially if local buckling is permitted. This erratic behavior is caused by abrupt changes in the mode shape corresponding to local buckling associated with small changes in the decision variables.

Simulation of a test of the optimized panel under increasing loads Nx, Nxy, p (Analysis type 3: ITYPE = 3); Stiffener spacing b = 8.0 inches

In this section are discussed results from the new "test simulation" branch of PANDA2 mentioned in Item 11 of "Improvements to PANDA2". The results for conditions at the midlength of the panel are given in Figs. 12 - 20. Those for conditions at the panel ends appear in Figs. 21 - 25. The starting (Nx, Nxy, p) are (-25, 25, 0.25) and the increments are (-25, 25, 0.25). Where the figures show plots of behavior vs axial load Nx, bear in mind that the in-plane shear load Nxy and normal pressure p are increasing in proportion to Nx. All of the results of this section were generated with all factors of safety set to unity.

CONDITIONS AT PANEL MIDLENGTH: Since the pressure bends the panel upward, as shown in the lower left portion of Fig. 4, the skin is compressed more than the stringer parts. One expects local buckling of the skin to occur at the panel midlength first.

Figure 12 shows buckling margins as functions of axial load Nx. Though negative margins at the design load corresponding to various types of local buckling appear in Fig. 12, they do not mean the design is unfeasible. The "test simulation" run was made with all factors of safety set to unity, whereas the final optimization runs were made with the factor of safety for local buckling, FSLOC, set equal to a number much less than unity so that local buckling constraints would not affect the evolution of the design. FSLOC was reset to unity in the "test simulation" run in order to generate plots which demonstrate that the design load corresponds to a locally postbuckled state.

Figure 13 shows the stress constraints vs. Nx. At the design load the maximum effective stress ("effective" in the sense of Von Mises) occurs at nodal point 6 in the panel skin (Segment 5, node 6: See Fig. 3). Probably the effective stress in the panel skin at the junction between Segment 2 and Segment 5 (Segment 5, node 1) is almost critical at the design load, since it represents the maximum stress anywhere in the panel cross section for axial compression less than 400 lb/in.

Figure 14 shows how the optimized cross section deforms at the panel midlength as the load combination Nx, Nxy, p is increased. Notice that for the optimized design there is little deformation in the stringer web or flange. This is because under the pressure acting from below, as shown in Fig. 4, the stringer web and flange are primarily in axial tension at the midlength of the panel. The maximum normal deflection in the skin occurs midway between stringers and is indeed large: wmax = 1.05 in. The skin deflection becomes especially large in the postbuckling regime because there are no rings (transverse stiffeners) that prevent excessive deepening of the local diagonal buckles as the in-plane shear load is increased. The postbuckling deformations are not antisymmetric about the skin-web intersection because the deformations caused by pressure are symmetric and the modal deformations are antisymmetric.

Figure 15 shows a "3-D" view of the locally postbuckled panel at the maximum load

applied in the "test simulation" run: (Nx, Nxy, p) = (-725 lb/in, 725 lb/in, 7.25 psi). The local buckling nodal lines are at an angle because of the in-plane shear loading Nxy. In the far postbuckled state the axial wavelength of the local buckles is long.

Figure 16 demonstrates the modification in PANDA2 mentioned in Item 14 in the section "Improvements to PANDA2". PANDA2 predicts bifurcation buckling with 5 axial halfwaves. As the panel is loaded into the postbuckling regime the number of axial halfwaves decreases in this case except for discontinuous behavior corresponding to axial loads Nx = -325 lb/in and Nx = -350 lb/in. The discontinuous behavior is caused by failure of convergence of the Item 14 modification. When this happens PANDA2 reverts to the original formulation described in [35]. Whether or not the lack of convergence of the new strategy for the two load steps indicates real lack of uniqueness of equilibrium states in the physical world (secondary bifurcation) might be determined by setting up and running a nonlinear finite element model with STAGS [21,22] or some other general-purpose code.

Figure 17 shows the growth in normal deflection midway between stringers and Fig. 18 shows the change in slope of the post-local-buckling nodal lines with increasing load. Figures 16 - 18 demonstrate that PANDA2 allows for changes in the local buckling pattern as the load is increased above the bifurcation load for local buckling.

Figure 19 shows the tangent stiffnesses of the combination of Segments 1 and 2 of the panel skin averaged for axial (CTAN(1,1)), hoop (CTAN(2,2)) and in-plane shear (CTAN(3,3)) loading. The tangent stiffnesses drop most rapidly in the neighborhood of the local bifurcation buckling load. These quantities play a role in the determination of the load factor for general instability and wide-column buckling of the locally postbuckled panel. The tangent stiffnesses drop before the bifurcation buckling load factor is reached because the amplitude of the initial imperfection (one tenth the skin thickness in this example) starts to grow steeply as the bifurcation buckling load factor is approached.

Figure 20 demonstrates the new capability of PANDA2 to generate plots of extreme fiber strains at user-selected points in the skin-stringer cross section. (See Item 16 in "Improvements to PANDA2). Analogous plots of axial and hoop strain are not included here in order to save space. The discontinuous behavior exhibited in Figs. 17 - 20 is generated as described in connection with Fig. 16.

CONDITIONS AT PANEL ENDS: As seen in Fig. 4 conditions at the panel ends are characterized by the stringer flanges being compressed more than the panel skin. Therefore, one might expect local buckling to be characterized by considerable deformation of the stringer cross section.

Figures 21 and 22 show design margins vs axial load Nx. In Fig. 21 there are three curves entitled "local buckling":

1. Local buckling: discrete model
2. Local buckling: Koiter theory
3. Local buckling: PANDA model

The first curve, Local buckling: discrete model, is too conservative in this case because the skin is in very slight axial compression or even axial tension combined with considerable in-plane shear. Because of the manner in which in-plane shear is accounted for in the BOSOR4-type discretized local buckling model (See the section "Philosophy embodied in PANDA2") the knockdown factor to account for the effect of in-plane shear loading is far too small. The third curve, Local buckling: PANDA model, is based on an incomplete model because it does not account for the stiffening effect of the thickened base beneath each stringer (width b2) nor for the behavior of the stringer cross section during buckling. The second curve, Local buckling: Koiter theory is the best model and actually governs the local postbuckling behavior in PANDA2. This theory uses the mode shape from the discretized BOSOR4 model and includes the in-plane shear load directly rather than indirectly by means of a knockdown factor.

Figure 22 shows the maximum effective stress vs. axial load Nx. The location of the critical stress is at the topmost fiber at the tip of the flange. The discontinuous behavior exhibited at the design load in Figs. 21 and 22 is caused by the change in number of axial halfwaves in the critical local buckling pattern from 2 to 3. At the optimum design the buckling load factors for 2 and 3 axial halfwaves are nearly the same.

Figures 23 and 24 show the locally deformed panel module cross section (Fig. 23) and one full axial wave of the buckling pattern (Fig. 24). The maximum deflection is less than a tenth of that at the panel midlength.

Figure 25 shows the in-plane shear strain at various points in the panel module cross section. The discontinuous behavior is caused by the change in number of axial half waves from 2 to 3.

Optimization (Analysis type 1: ITYPE = 1) with stringer spacing b permitted to change

Figures 26 - 32 are plots of the objective (panel weight), design variables, and design margins v. optimization iterations. The starting design used here is the final design just discussed. The case was run in the following way:

1. The DECIDE processor (see "Architecture" section) was rerun with all dimensions shown in Fig. 4 chosen as decision variables. In addition, the width of the

thickened base under each stringer (dimension b2 in Fig. 4) is not permitted to be wider than one third of the stringer spacing (b2 < b/3).

2. All "PANDAOPT" runs were made with IQUICK = 0 and with FSLOC = 0.1 (local buckling permitted).

3. There were 9 "PANDAOPT" runs in which a maximum of 5 iterations/run was permitted and 4 "PANDAOPT" runs in which a maximum of 25 iterations/run was permitted.

Figure 26 shows the evolution of the objective. The panel becomes significantly lighter when the stringer spacing b is permitted to vary during optimization cycles. Figures 27 and 28 show the evolution of the panel module cross section dimensions. The stringer spacing decreases until it reaches the user-specified lower bound of 2.5 inches. The thicknesses of the various segments decrease. There are less dramatic changes in the height h of the web and width w of the outstanding flange.

The following observations pertain to conditions at the midlength of the panel (Figs. 29 and 30):

1. In contrast to the previous case in which stringer spacing b was held at 8.0 inches (Fig. 8), the wide-column and general instability modes of failure now become critical (Fig. 29).

2. Critical and near-critical stresses occur at several locations in the panel module cross section (Fig. 30). (Compare with Fig. 9).

The following observations pertain to conditions at the ends of the panel (Figs. 31 and 32):

1. Several kinds of buckling that involve deformation of the stringer cross section become critical (Fig. 31). (Compare with Fig. 10).

2. Stresses are not critical (Fig. 32). (Compare with Fig. 11).

Simulation of a test of the optimized panel under increasing loads Nx, Nxy, p (Analysis type 3: ITYPE = 3); Stiffener spacing b = 2.5 inches

The results for conditions at the midlength of the panel appear in Figs. 33 - 35 and the results for conditions at the ends of the panel appear in Figs. 36 - 38. All the results of this section were obtained with the factor of safety for local buckling, FSLOC, set equal to unity.

CONDITIONS AT THE PANEL MIDLENGTH: Figure 33 shows the buckling margins. At the design load the optimized panel is loaded well into its locally postbuckled state. (Compare Fig. 33 with Fig. 12). Figure 34 shows how the panel module cross section deforms in the post-local-buckling regime. The maximum deflection is much less than in the previous case in which b = 8.0 inches. (Compare Fig. 34 with Fig. 14). Figure 35 shows a "3-D" plot analogous to that in Fig. 15. The postbuckling axial wavelength is much shorter and the slope of the nodal lines of the local buckles is less.

CONDITIONS AT THE PANEL ENDS: Figure 36 shows the buckling margins. The PANDA model indicates that the skin is in its locally postbuckled state at the design load. However, this model is too conservative because it does not account for the stiffening effects of the thickened base under the stringer or the stringer itself. The local buckling margin as predicted by the Koiter theory, which accounts for these stiffening effects, governs here. It shows that the skin is not in its locally postbuckled state at the design load. (Compare Fig. 36 with Fig. 21). Figure 37 shows how the panel module cross section deforms in the locally postbuckled regime. The deflection in the panel skin, symmetric about the stringer, is caused entirely by the normal pressure in this case. Buckling of the stringer web and flange has a short axial wavelength (23 halfwaves over the 30-inch length of the panel). In the example with stringer spacing fixed at 8.0 inches the buckling mode was characterized by stringer sidesway with a rather long axial wavelength (2 waves over the 30-inch length of the panel. (Compare Fig. 37 and Fig. 23). Figure 38 shows a "3-D" plot of the local buckling mode at the panel ends. (Compare Fig. 38 and Fig. 24).

## COMPARISONS WITH RESULTS FROM STAGS [21,22]

Currently an effort is underway to produce automatically input data for the STAGS computer program from output data from PANDA2. Figure 39 shows an example of the optimized, locally buckled T-stiffened panel for the case in which the stringer spacing b is fixed at 8.0 inches. The finite element model shown in Fig. 39 was generated by a new PANDA2 processor called STAGSMODEL. Wheras PANDA2 predicts local buckling at the midlength of the panel at (Nx, Nxy, p) = (-125, 125, 1.25), STAGS predicts local buckling at (Nx, Nxy, p) = (-132, 132, 1.32), a discrepancy of less than six percent. Most of the difference can be attributed to the fact that for the purpose of the calculation of local buckling, PANDA2 assumes that the prebuckling conditions at the midlength of the panel extend infinitely in the axial direction. PANDA2 predicts local buckling with an axial half-wavelength of six inches and slope of buckling nodal lines equal to 0.343. While it is difficult to tell exactly what the slope of the buckling nodal lines is in Fig. 39, it appears that with respect to the local buckling mode shape PANDA2 and STAGS are in reasonably good agreement.

Work is continuing to produce STAGS results for the nonlinear response of the panel as the load combination is increased. Difficulties in the STAGS analysis associated with mode jumping have been encountered.

## CONCLUSIONS

This example demonstrates various phenomena that occur when a panel clamped at its ends is subjected to combined in-plane loads and normal pressure. New postprocessing features of PANDA2 are demonstrated.

In optimized panels in which local buckling is permitted during service:

1. At the midlength of the panel the design is constrained by high stresses developing in the skin and possibly by general instability (depending on the stringer spacing).
2. At the ends of the panel the design is constrained by a multitude of stringer buckling modes and possibly by high stresses that develop in the various stringer segments.

Cases similar to those discussed here but with rings present should be run. The rings (transverse stiffeners) would prevent the very large normal deflections seen in Fig. 14 from developing when there is significant in-plane shear loading. Cases involving laminated composite materials should be explored.

## ACKNOWLEDGMENTS

The author is indeed grateful for the continuing support of Mr. Bill Sable and Mr. Stan Simson, Stress and Fractural Mechanics Department in Lockheed Missiles and Space Company's Satellite Systems Division.

The results plotted in Figs. 5 - 38 were obtained on the DEC 5000 workstation with the UNIX version of PANDA2. PANDA2 was converted from operation on VAX computers with the VMS operating system to operation on DEC and SUN computers with UNIX operating systems. The conversion was performed by Bill D. Bushnell. The plots were produced via a plot package written by Bill Bushnell for operation on any printer with a POSTSCRIPT capability.

Harold Cabiness, Charles Rankin, and Frank Brogan helped the writer come up to speed on STAGS, and Harold Cabiness and Bo Stehlin taught the writer how to produce plots such as that shown in Fig. 39 via the PATRAN system.

Mary Ellen Hasbrouck produced the final version of Fig. 4.

## REFERENCES

[1] A. W. Leissa, ''Buckling of laminated composite plates and shell panels," AFWAL-TR-85-3069, Air Force Wright Aeronautical Laboratories, Wright-Patterson AFB, Ohio 45433, June, 1985.

[2] J. F. M. Wiggenraad, ''Postbuckling of thin-walled composite structures - design, analysis, and experimental verification," National Aerospace Laboratory (NLR), The Netherlands, Memorandum SC-86-013 U, Feb. 28, 1986.

[3] R. R. Arnold and J. C. Parekh, ''Buckling, postbuckling, and failure of flat and shallow-curved, edge-stiffened composite plates subject to combined axial compression and shear loads", Presented at 27th SDM Meeting, San Antonio, Tx., April 1986, AIAA Paper No. 86-1027-CP, 1986, Proceedings pp. 769-782.

[4] D. Bushnell, ''PANDA-Interactive program for minimum weight design of stiffened cylindrical panels and shells,'' Computers and Structures, 16, 1983, pp. 167-185.

[4b] D. Bushnell, ''Theoretical basis of the PANDA computer program for preliminary design of stiffened panels under combined in-plane loads," Computers and Structures, Vol. 27, No. 4, pp 541-563 (1987)

[5] D. Bushnell, Computerized Buckling Analysis of Shells, Martinus Nijhoff Publishers, The Netherlands, 1985.

[6] M. Baruch and J. Singer, ''Effect of eccentricity of stiffeners on the general instability of stiffened cylindrical shells under hydrostatic pressure," Journal of Mechanical Engineering Science, 5, (1) (1963) pp.23-27.

[7] J. H. Starnes,Jr., N. F. Knight,Jr. and M. Rouse, ''Postbuckling behavior of selected flat stiffened graphite- epoxy panels loaded in compression,'' AIAA Paper 82-0777, presented at AIAA 23rd Structures, Structural Dynamics, and Materials Conference, New Orleans, May, 1982. See also, AIAA J., 23, (8) (1985) pp.1236-1246.

[8] E. E. Spier, ''On experimental versus theoretical incipient buckling of narrow graphite/epoxy plates in compression," Proc. AIAA 21st SDM Conference, AIAA Paper 80-0686-CP, May, 1980.

[9] E. E. Spier, ''Local buckling, postbuckling, and crippling behavior of graphite-epoxy short thin-walled compression members," Naval Air Systems Command, Washington, D. C., NASC-N00019-80-C-0174, July 1981.

[10] M. P. Renieri and R. A. Garrett, ''Investigation of the local buckling, postbuckling and crippling behavior of graphite/epoxy short thin-walled compression members," McDonnell Douglas Corporation, St. Louis, Missouri, MDC A7091, July 1981.

[11] M. P. Renieri and R. A. Garrett, ''Postbuckling fatigue behavior of flat stiffened graphite/epoxy panels under shear loading," Naval Air Development Center, Warminster, PA, NADC-81-168-60, July 1982.

[12] L. W. Rehfield and A. D. Reddy, ''Observations on compressive local buckling, postbuckling, and crippling of graphite/epoxy airframe structure," Proc. 27th AIAA SDM Conference, AIAA Paper 86-0923-CP, May 1986.

[13] T. Weller, G. Messer and A. Libai, ''Repeated buckling of graphite epoxy shear panels with bonded metal stiffeners," Dept. of Aeronautical Engineering, Technion, Haifa, Israel, TAE No. 546, August 1984.

[14] B. L. Agarwal, ''Postbuckling behavior of composite, stiffened, curved panels loaded in compression," Experimental Mechanics, Vol. 22, June 1982.

[15] C. Blaas and J. F. M. Wiggenraad, ''Development and test verification of the ARIANE 4 interstage 2/3 in CFRP", Proceedings of the AIAA/ASME 27th Structures, Structural Dynamics and Materials Conference, Part 1, May 1986, pp. 307-313.

[16] J. M. T. Thompson, J. D. Tulk and A. C. Walker, ''An experimental study of imperfection-sensitivity in the interactive buckling of stiffened plates", in: Buckling of Structures, B. Budiansky, ed., Springer-Verlag, 1976, pp 149-159.

[17] Bushnell, D., Holmes, A.M.C, Flaggs, D.L., and McCormick, P.J., ''Optimum design, fabrication, and test of graphite-epoxy, curved, stiffened, locally buckled panels loaded in axial compression,'', in BUCKLING OF STRUCTURES, edited by I. Elishakoff, et al, Elsevier Science Publishers, Amsterdam, pp 61-131 (1988)

[18] N. R. Bauld, Jr. and N. S. Khot, ''A numerical and experimental investigation of the buckling behavior of composite panels", Computers and Structures, 15 (1982) pp. 393-403.

[19] N. S. Khot and N. R. Bauld, Jr., ''Further comparison of the numerical and experimental buckling behaviors of composite panels," Computers and Structures, 17, (1983) pp. 61-68.

[20] Y. Zhang and F. L. Matthews, ''Postbuckling behavior of anisotropic laminated plates under pure shear and shear combined with compressive loading", AIAA Journal, 22, (2), (1984) pp 281-286.

[21] B. O. Almroth and F. A. Brogan, ''The STAGS Computer Code", NASA CR-2950, Nasa Langley Research Center, Hampton, Va., 1978.

[22] C. C. Rankin, P. Stehlin and F. A. Brogan, ''Enhancements to the STAGS computer code", NASA CR 4000, NASA Langley Research Center, Hampton, Va, November 1986. See also, G. A. Thurston, F. A. Brogan and P. Stehlin, ''Postbuckling analysis using a general purpose code", AIAA Journal, 24, (6) (1986) pp. 1013-1020.

[23] Graves-Smith, T.R. and Sridharan, S., ''A finite strip method for the post-locally-buckled analysis of plate structures,'' Int. J. Mech. Sci., Vol. 20, pp 833-843 (1978)

[24] Stoll, F. and Gurdal, Z., ''Nonlinear analysis of compressively loaded linked-plate structures,'' AIAA Paper 90-0968-CP, Proceedings 31st AIAA/ASME Structures, Structural Dynamics, and Materials Meeting, pp 903-913

[25] Riks, E., ''A finite strip method for the buckling and postbuckling analysis of stiffened panels in wing box structures,'' National Aerospace Laboratory (NLR), Report NLR CR 89383 L, The Netherlands, November 1989

[26] M. S. Anderson and W. J. Stroud, ''General panel sizing computer code and its application to composite structural panels,'' AIAA Journal, 17, (8) (1979) pp. 892-897.

[27] W. J. Stroud and M. S. Anderson, ''PASCO: Structural panel analysis and sizing code, capability and analytical foundations,'' NASA TM-80181, NASA Langley Research Center, Hampton, Va., 1981.

[28] W. J. Stroud, W. H. Greene and M. S. Anderson, ''Buckling loads of stiffened panels subjected to combined longitudinal compression and shear: Results obtained with PASCO, EAL, and STAGS computer programs,'' NASA TP 2215, Nasa Langley Research Center, Hampton, Va., January 1984.

[29] J. N. Dickson, R. T. Cole and J. T. S. Wang, ''Design of stiffened composite panels in the post-buckling range," in: Fibrous Composites in Structural Design, E. M. Lenoe, D. W. Oplinger, and J. J. Burke, editors, Plenum Press, New York, 1980, pp 313-327.

[30] J. N. Dickson, S. B. Biggers, and J. T. S. Wang, ''Preliminary design procedure for composite panels with open-section stiffeners loaded in the post-buckling range," in: Advances in Composite Materials, A. R. Bunsell, et al,editors, Pergamon Press Ltd., Oxford, England, 1980, pp 812-825.

[31] J. N. Dickson and S. B. Biggers, ''POSTOP: Postbuckled open- stiffened optimum panels, theory and capability", NASA Langley Research Center, Hampton, Va., NASA Contractor Report from NASA Contract NAS1 - 15949, May 1982.

[32] Butler, R. and Williams, F. W., ''Optimuam design features of VICONOPT, an exact buckling program for prismatic assemblies of anisotropic plates,'' AIAA Paper 90-1068-CP, Proceedings 31st AIAA/ASME Structures, Structural Dynamics, and Materials Meeting, pp 1289-1299

[33] Williams, F. W., Kennedy, D., Anderson, M.S., ''Analysis features of VICONOPT, an exact buckling and vibration program for prismatic assemblies of anisotropic plates,'', AIAA Paper 90-0970-CP, Proceedings 31st AIAA/ASME Structures, Structural Dynamics, and Materials Meeting, pp 920-929

[34] Peng, M-H and Sridharan, S., ''Optimized design of stiffened panels subject to interactive buckling,'' AIAA Paper 90-1067-CP, Proceedings 31st AIAA/ASME Structures, Structural Dynamics, and Materials Meeting, pp 1279-1288

[35] D. Bushnell, ''PANDA2-Program for minimum weight design of stiffened, composite, locally buckled panels", Computers and Structures, Vol. 25 (1987) pp. 469-605. See also, D. Bushnell, ''Use of PANDA2 to optimize composite, imperfect, stiffened, locally buckled panels under combined in-plane loads and normal pressure," in DESIGN AND ANALYSIS OF COMPOSITE MATERIAL VESSELS, PVP Vol. 121, pp 21-42, ASME, 1987

[36] G. N. Vanderplaats, ''CONMIN-a FORTRAN program for constrained function minimization,'' NASA TM X 62-282, version updated in March, 1975, Ames Research Center, Moffett Field, CA (Aug.1973) See also, G. N. Vanderplaats and F. Moses, ''Structural optimization by methods of feasible directions,'' Computers and Structures, 3 (1973) pp. 739-755.

[37] Vanderplaats, G. N., "ADS--a FORTRAN program for automated design synthesis, Version 2.01", Engineering Design Optimization, Inc, Santa Barbara, CA, January, 1987

[38] Vanderplaats, G. N. and Sugimoto, H., "A general-purpose optimization program for engineering design", Computers and Structures, Vol. 24, pp 13-21, 1986

[39] D. Bushnell, ''BOSOR4: Program for stress, buckling, and vibration of complex shells of revolution,'' Structural Mechanics Software Series - Vol. 1, (N. Perrone and W. Pilkey, editors), University Press of Virginia, Charlottesville, 1977, pp. 11-131. See also Computers and Structures, Vol. 4, (1974) pp. 399-435; AIAA J, Vol. 9, No. 10, (1971) pp. 2004-2013; Structural Analysis Systems, Vol. 2, A. Niku-Lari, editor, Pergamon Press, Oxford, 1986, pp. 25-54, and Computers and Structures, 18, (3), (1984) pp. 471-536.

[40] W. T. Koiter, ''Het Schuifplooiveld by Grote Overshrijdingen van de Knikspanning,'' Nationaal Luchtvaart Laboratorium, The Netherlands, Report X295, November 1946 (in Dutch)

[41] Bushnell, D., "Improvements to PANDA2", May 1989, revised December 1989, unpublished "handout" distributed with PANDA2

[42] Bushnell, D., "Truss-core sandwich design via PANDA2", AIAA Paper 90-1070-CP, Proceedings 31st AIAA/ASME Structures, Structural Dynamics, and Materials Meeting, pp 1313-1332

[43] Roark, R. J., FORMULAS FOR STRESS AND STRAIN, 3rd Edition, McGraw-Hill, 1954 (in particular Table III, Formula 33)

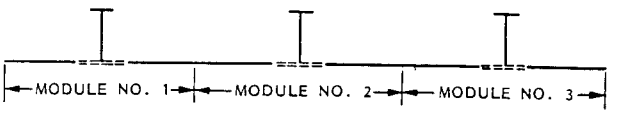


Fig. 1 TEE-stiffened panel with three modules

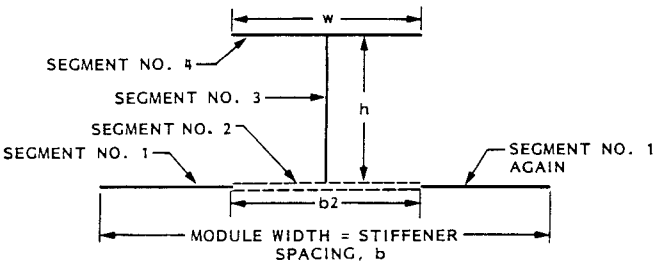


Fig. 2 A single panel module

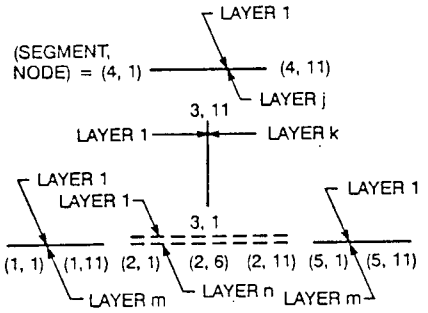


Fig. 3 Segment and nodal point numbering and layer numbering convention for a single panel module

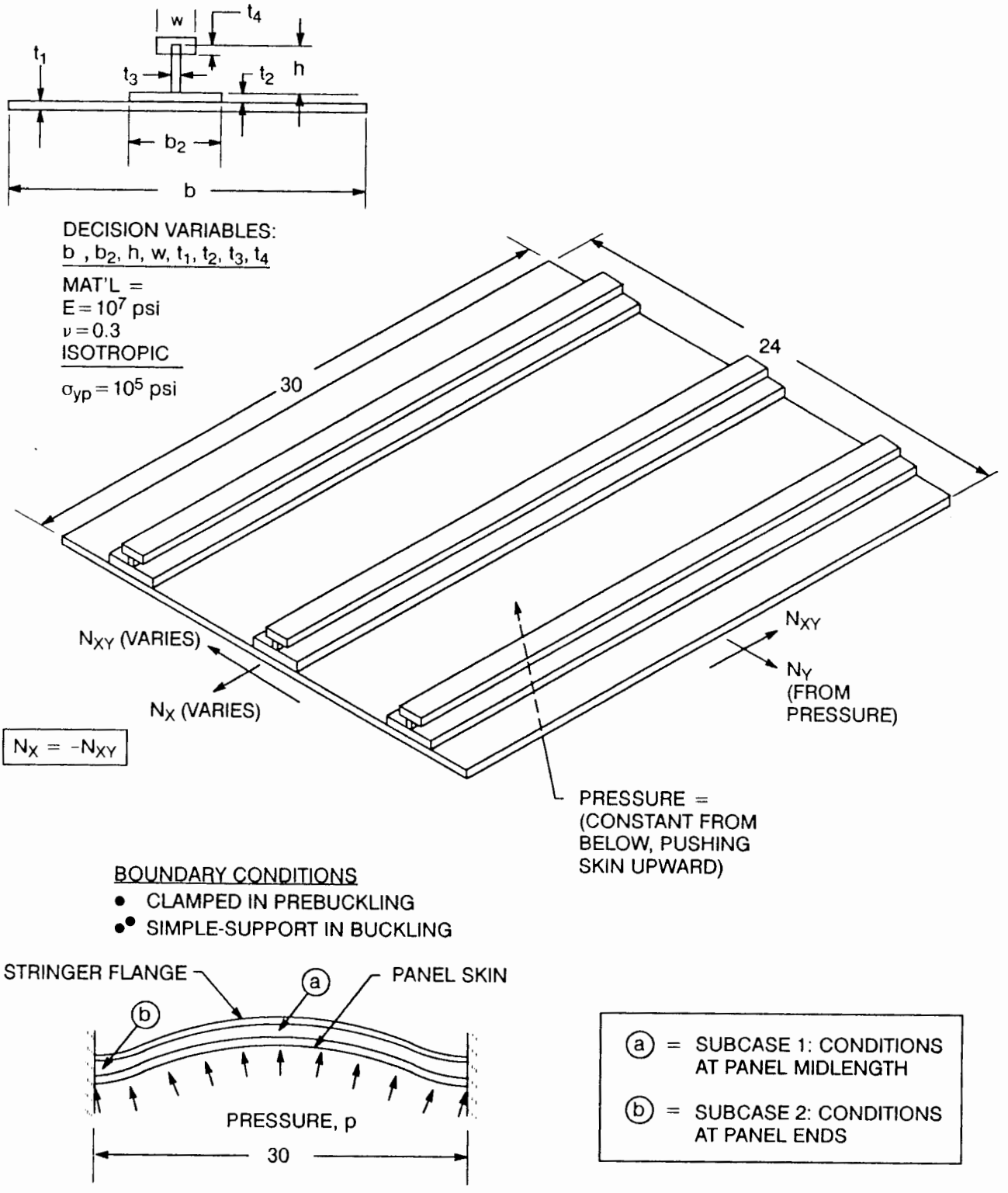


Fig. 4 Panel geometry, material properties, and loading

Table 1 Input data for the BEGIN processor of PANDA2

```
     N          $ Do you want a tutorial session and tutorial output?
    30          $ Panel length normal to the plane of the screen, L1
    24          $ Panel length in the plane of the screen, L2
     T          $ Identify type of stiffener along L1    (N, T, J, R, A)
     8          $ stiffener spacing, b
 2.000000       $ width of stiffener base, b2 (must be > 0, see Help)
 1.400000       $ height of stiffener (type H for sketch), h
 1.200000       $ width of outstanding flange of stiffener, w
     N          $ Are the stringers cocured with the skin?
 10000          $ What force/(axial length) will cause web peel-off?
     N          $ Is the next group of layers to be a "default group" (12 layers
     1          $ number of layers in the next group in Segment no.( 1)
     N          $ Can winding (layup) angles ever be decision variables?
     1          $ layer index (1,2,...), for layer no.( 1)
     Y          $ Is this a new layer type?
0.1000000       $ thickness for layer index no.( 1)
     0          $ winding angle (deg.) for layer index no.( 1)
     1          $ material index (1,2,...) for layer index no.( 1)
     N          $ Any more layers or groups of layers in Segment no.( 1)
     N          $ Is the next group of layers to be a "default group" (12 layers
     2          $ number of layers in the next group in Segment no.( 2)
     N          $ Can winding (layup) angles ever be decision variables?
     2          $ layer index (1,2,...), for layer no.( 1)
     Y          $ Is this a new layer type?
0.1000000       $ thickness for layer index no.( 2)
     0          $ winding angle (deg.) for layer index no.( 2)
     1          $ material index (1,2,...) for layer index no.( 2)
     1          $ layer index (1,2,...), for layer no.( 2)
     N          $ Is this a new layer type?
     N          $ Any more layers or groups of layers in Segment no.( 2)
     N          $ Is the next group of layers to be a "default group" (12 layers
     1          $ number of layers in the next group in Segment no.( 3)
     N          $ Can winding (layup) angles ever be decision variables?
     3          $ layer index (1,2,...), for layer no.( 1)
     Y          $ Is this a new layer type?
0.1000000       $ thickness for layer index no.( 3)
     0          $ winding angle (deg.) for layer index no.( 3)
     1          $ material index (1,2,...) for layer index no.( 3)
     N          $ Any more layers or groups of layers in Segment no.( 3)
     N          $ Is the next group of layers to be a "default group" (12 layers
     1          $ number of layers in the next group in Segment no.( 4)
     N          $ Can winding (layup) angles ever be decision variables?
     4          $ layer index (1,2,...), for layer no.( 1)
     Y          $ Is this a new layer type?
0.1000000       $ thickness for layer index no.( 4)
     0          $ winding angle (deg.) for layer index no.( 4)
     1          $ material index (1,2,...) for layer index no.( 4)
     N          $ Any more layers or groups of layers in Segment no.( 4)
     0          $ choose external (0) or internal (1) stringers
     N          $ Identify type of stiffener along L2  (N, T, J, R, A)
     N          $ Is the panel curved in the plane of the screen (Y for cyls.)?
     N          $ Is panel curved normal to plane of screen? (answer N)
     Y          $ Is this material isotropic (Y or N)?
0.1000000E+08   $ Young's modulus,                E( 1)
0.3000000       $ Poisson's ratio,               NU( 1)
 3846000.       $ transverse shear modulus,     G13( 1)
     0          $ Thermal expansion coeff.,   ALPHA( 1)
     0          $ residual stress temperature (positive),TEMPTUR( 1)
     N          $ Want to supply a stress-strain "curve" for this mat'l? (N)
     Y          $ Want to specify  maximum effective stress ?
 100000.0       $ Maximum allowable effective stress in material type( 1)
0.1000000       $ weight density (greater than 0!) of material type( 1)
     N          $ Is this unidirectional composite material (tape) ?
     1          $ Prebucking phase: choose 0=simple support or 1 = clamping
     1          $ Buckling phase: choose 0=simple support or 1=clamping
```

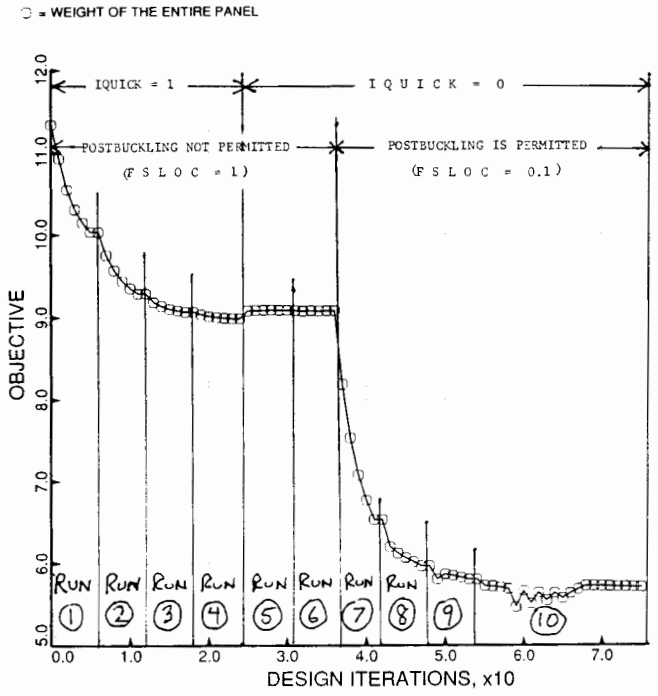


Fig. 5 Panel weight vs. iterations (b=8 in.)

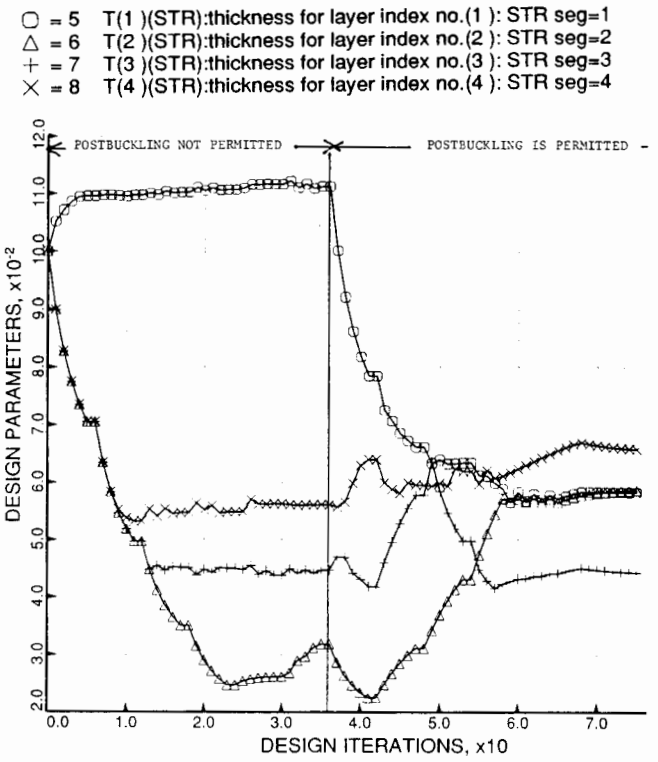


Fig. 7 Module layer thicknesses (b=8 in.)

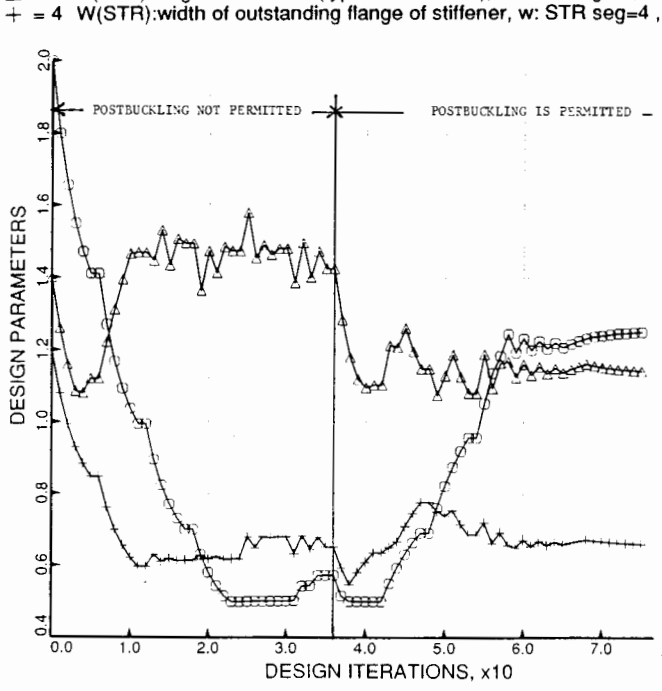


Fig. 6 Module segment widths (b=8 in.)

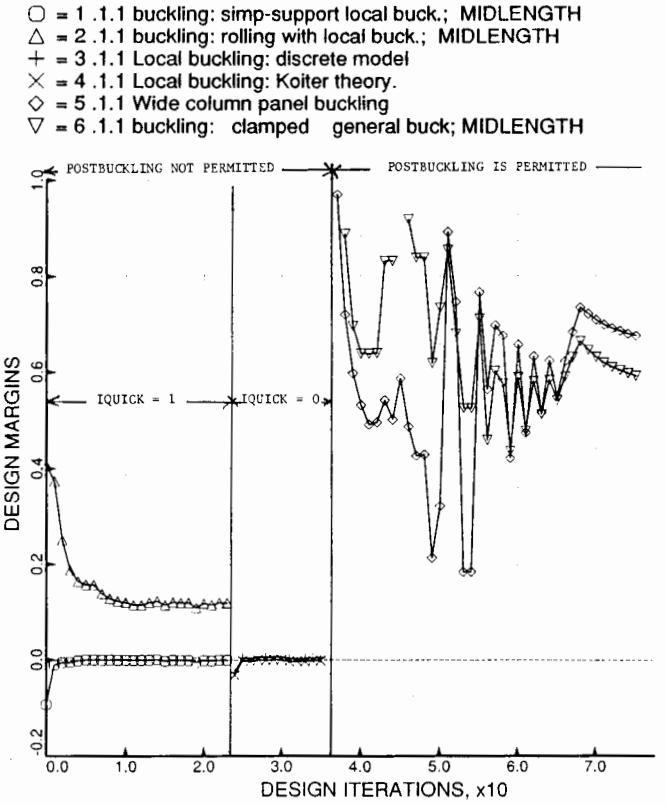


Fig. 8 Buckling margins, panel midlength, b=8 in.

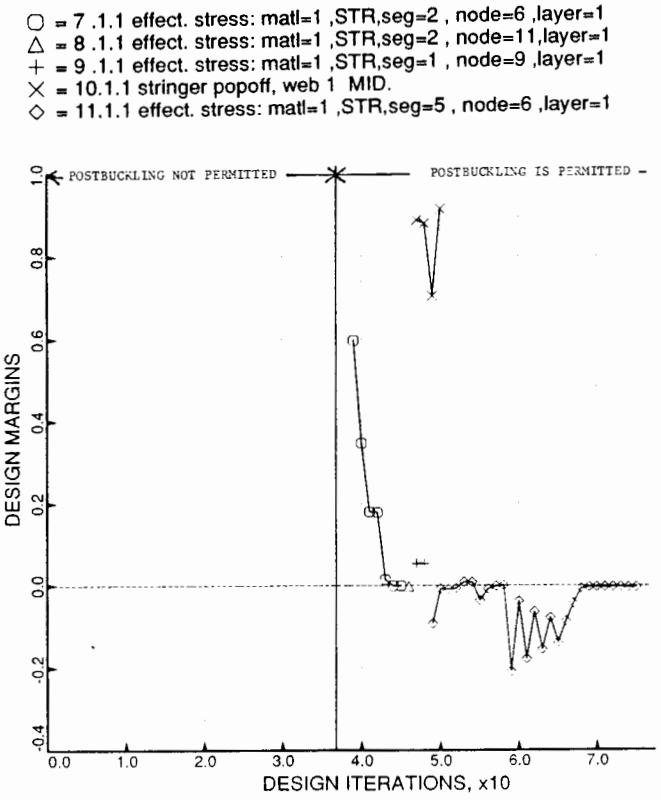


Fig. 9 Stress margins, panel midlength, b=8

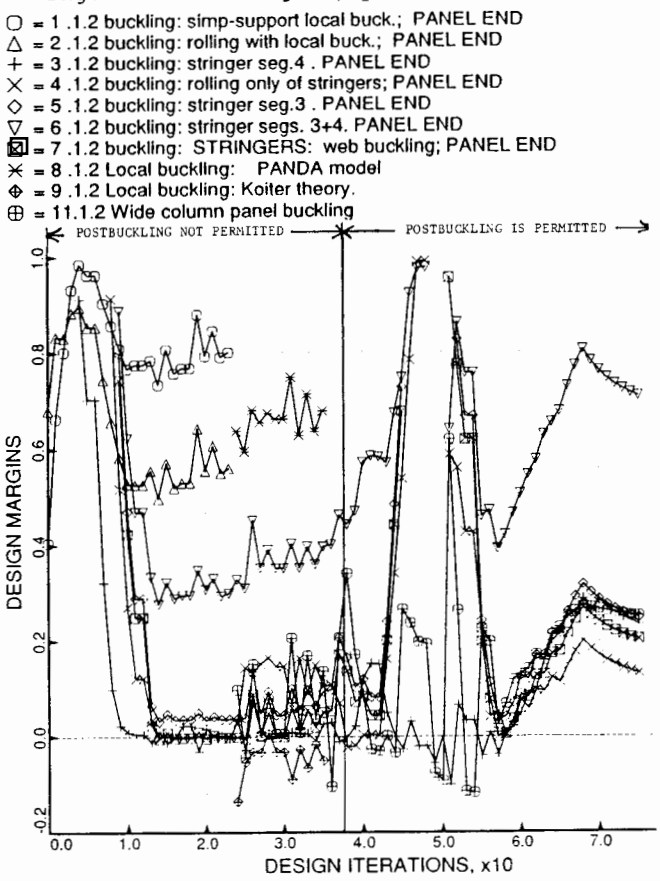


Fig. 10 Buckling margins, panel ends, b=8 in.

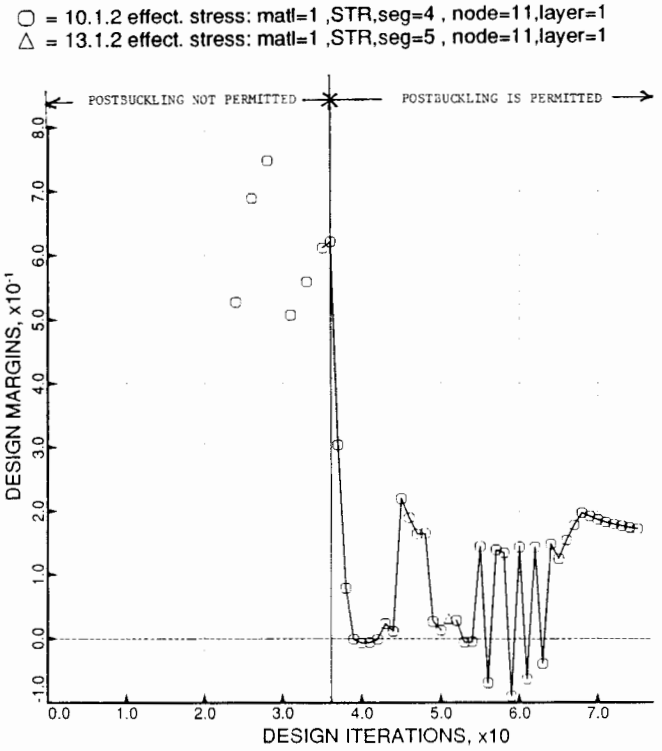


Fig. 11 Stress margins, panel ends, b=8 in.

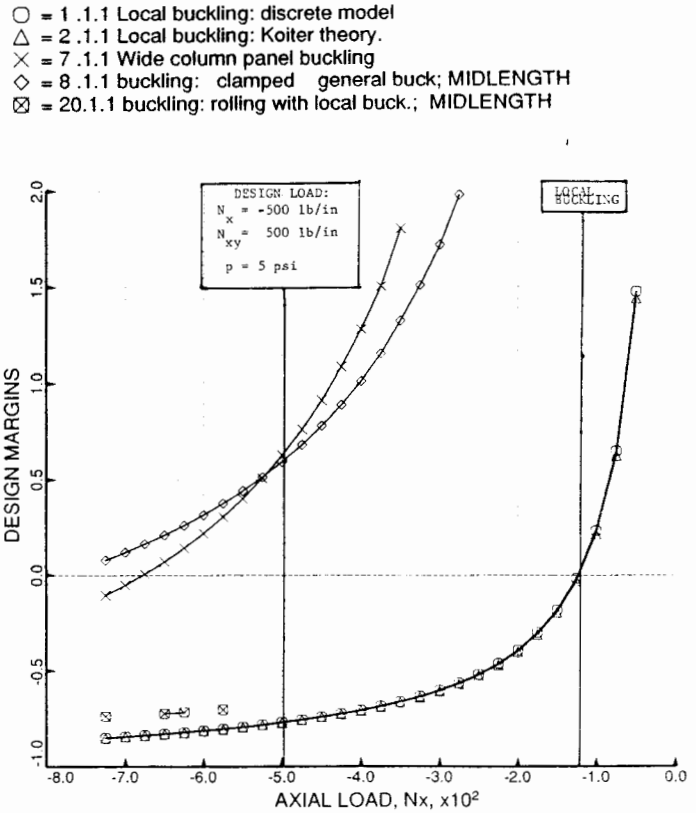


Fig. 12 Buckling margins, panel midlength, b=8 in., test simulation run

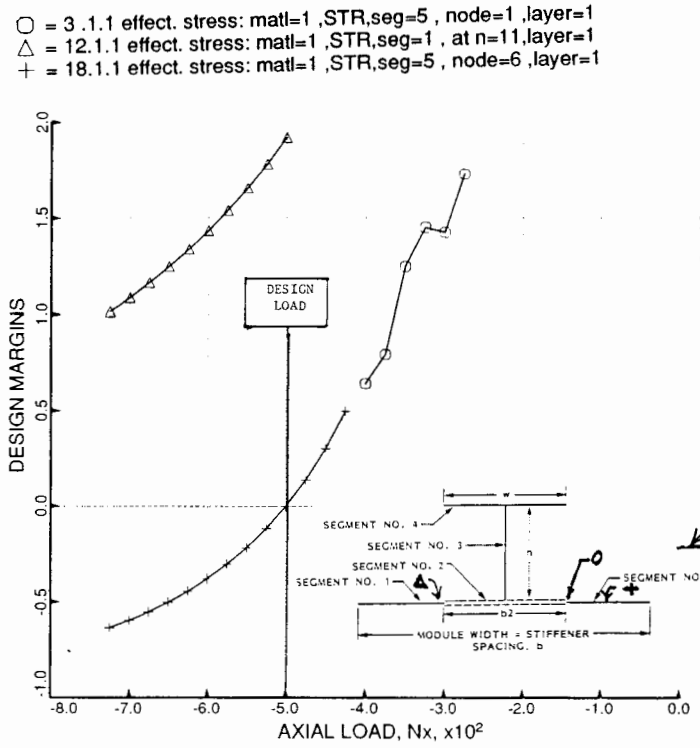


Fig. 13 Stress margins, panel midlength, b=8 in., test simulation run

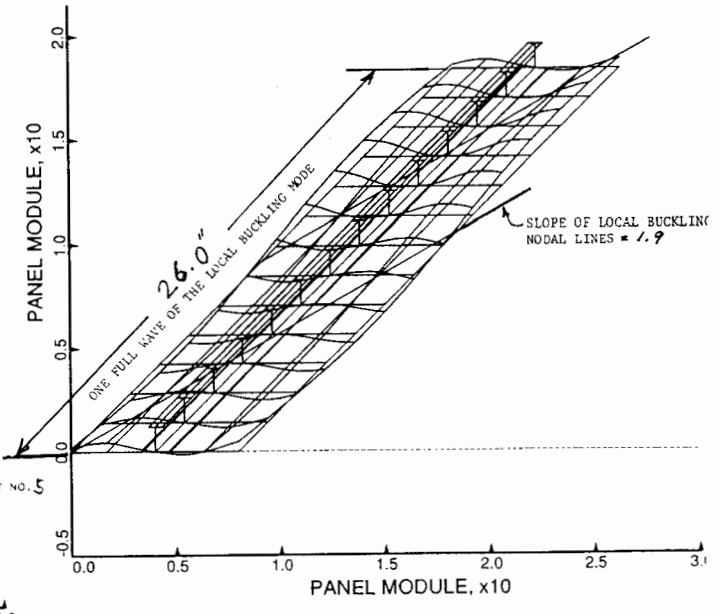


Fig. 15 Module deformation, panel midlength, b=8 in., test simulation run, 3-D view

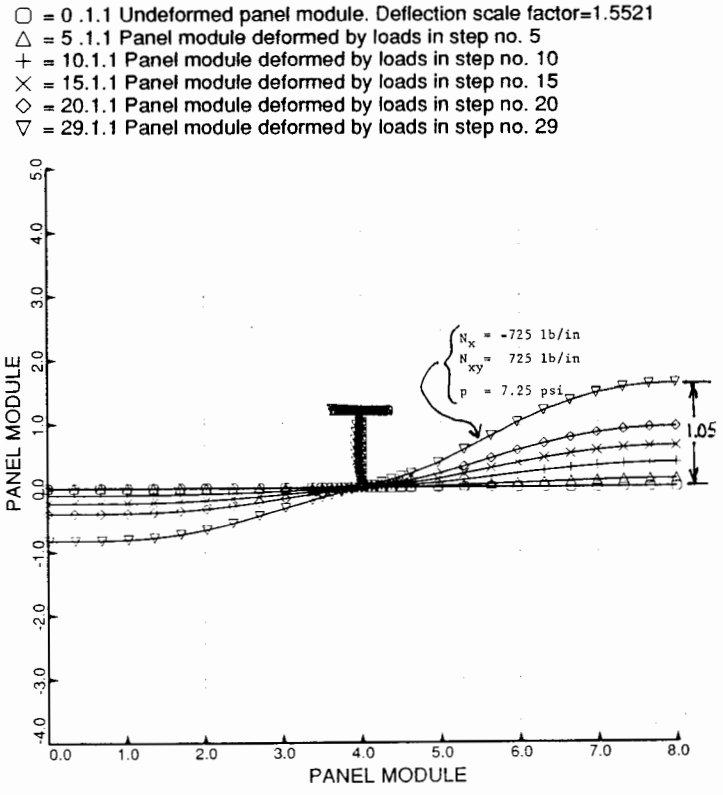


Fig. 14 Module deformation, panel midlength, b=8 in., test simulation run

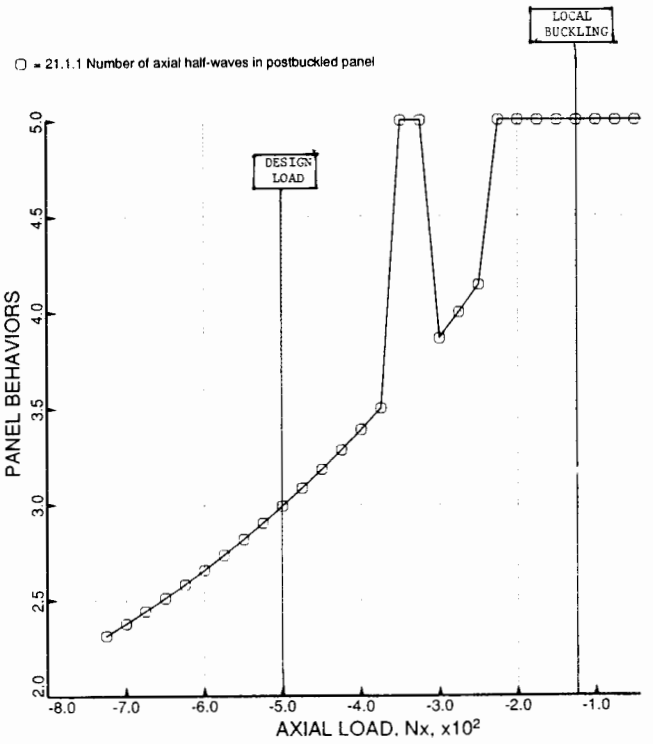


Fig. 16 Axial halfwaves v. load, midlength b=8 in., test simulation run

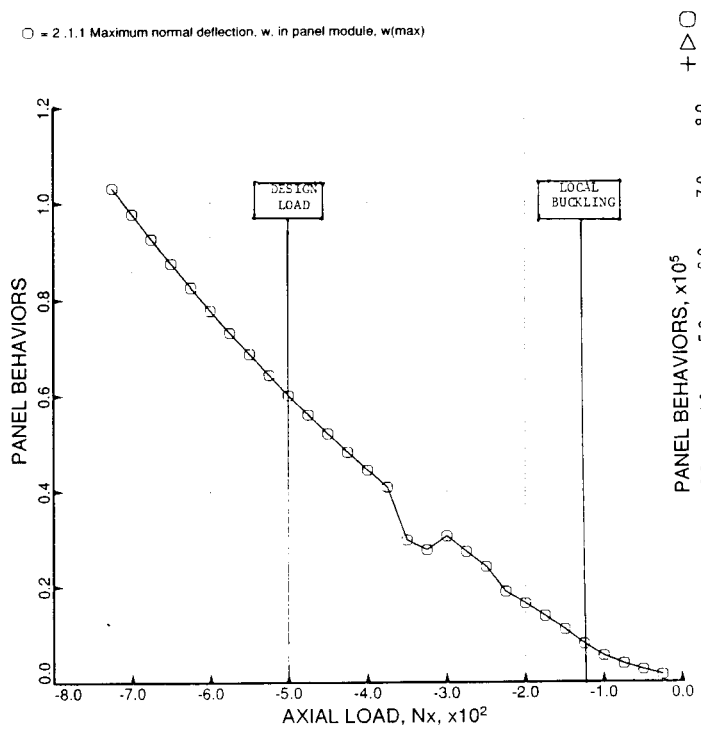


Fig. 17 Normal deflection in panel skin, panel midlength, b=8 in.

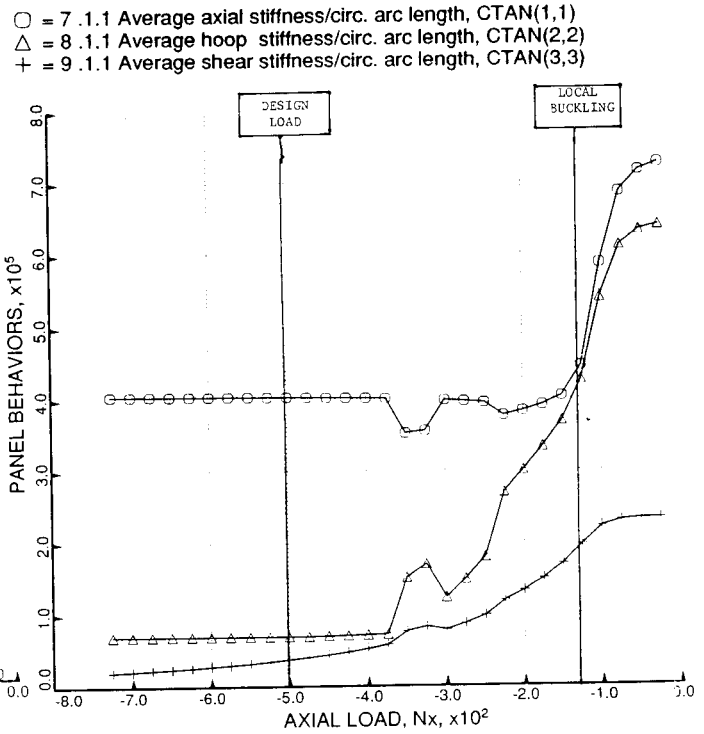


Fig. 19 Postbuckled panel skin stiffnesses, panel midlength, b=8 in.

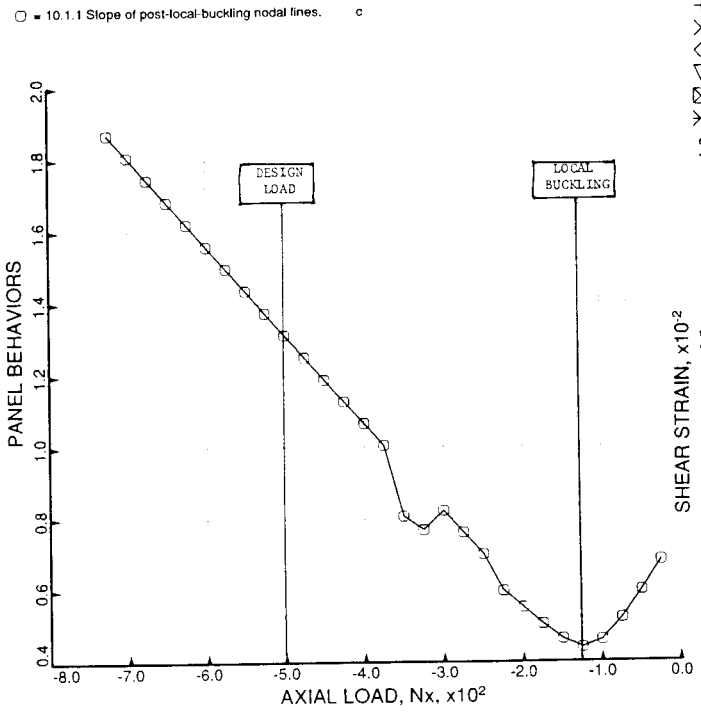


Fig. 18 Slope of buckling nodal lines, panel midlength, b=8 in.

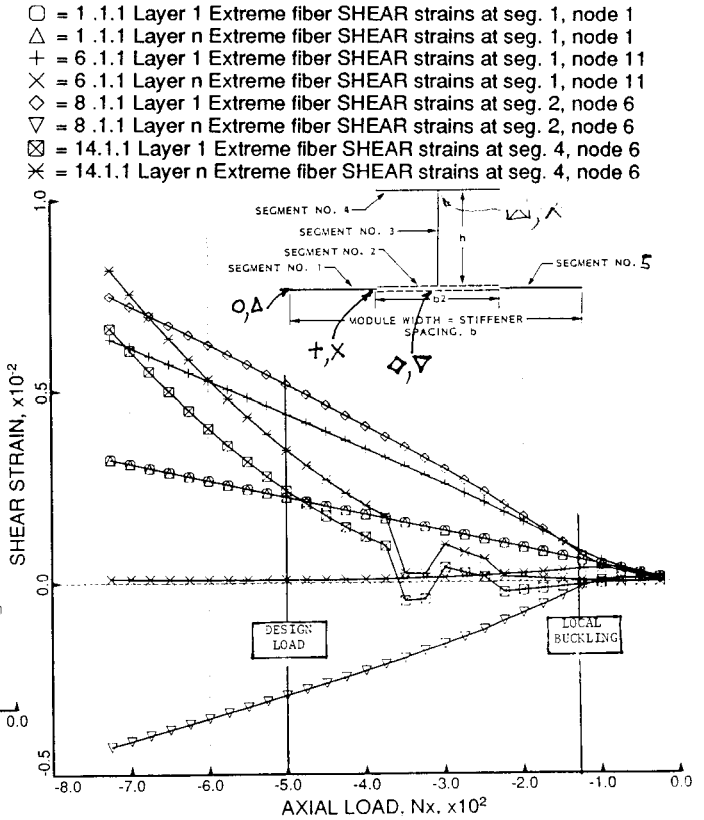


Fig. 20 Extreme fiber shear strains panel midlength, b=8 in.

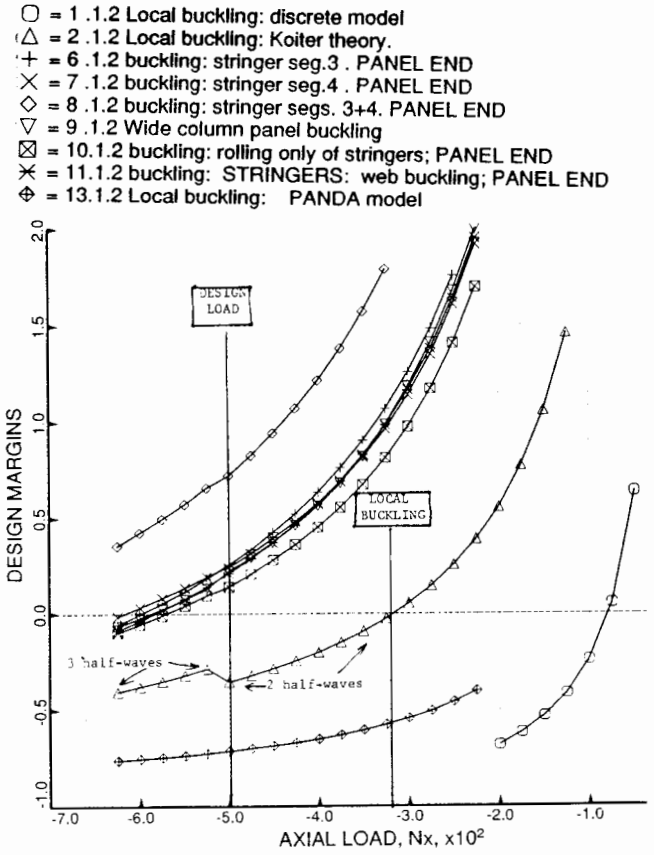


Fig. 21 Buckling margins, panel ends, b=8 in., test simulation run

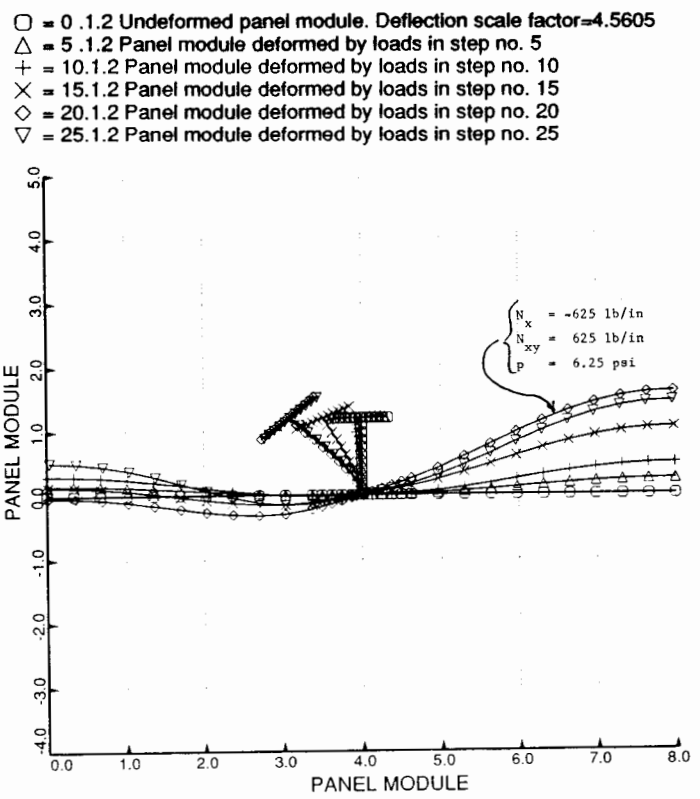


Fig. 23 Module deformation, panel ends, b=8 in., test simulation run

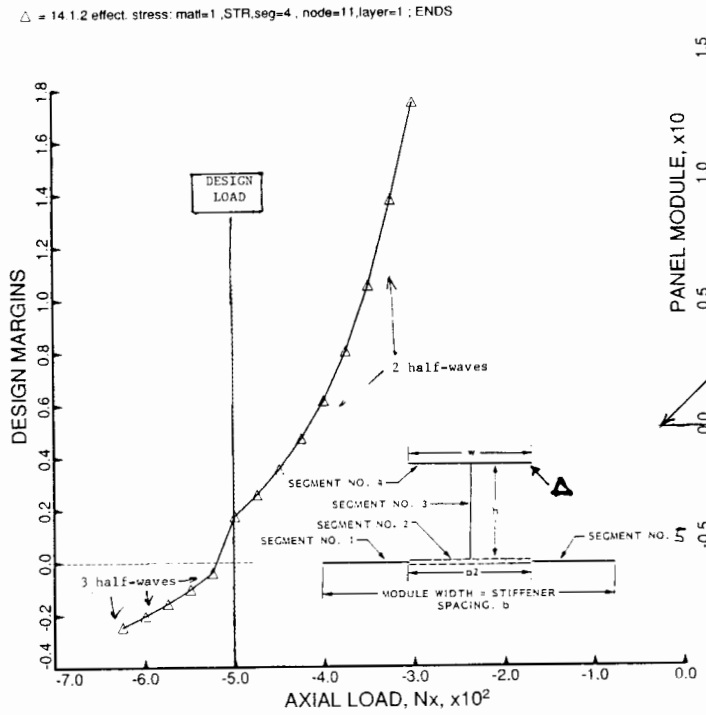


Fig. 22 Stress margins, panel ends, b=8 in., test simulation run

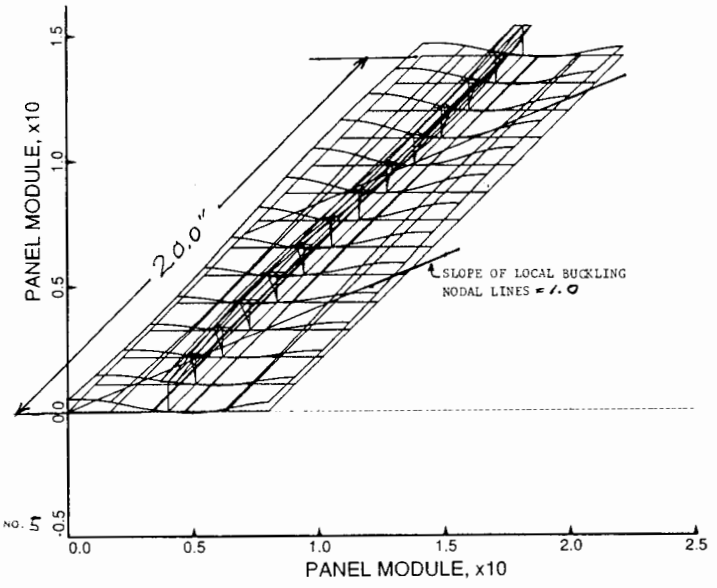


Fig. 24 Module deformation, panel ends, b=8 in., test simulation, 3-D

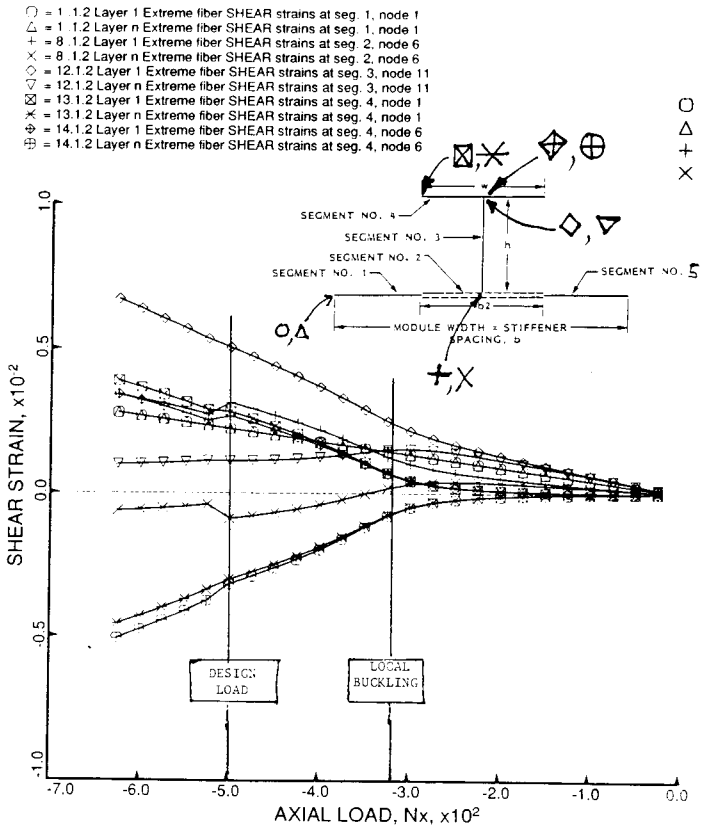


Fig. 25 Extreme fiber strains v. load, panel ends, b=8 in.

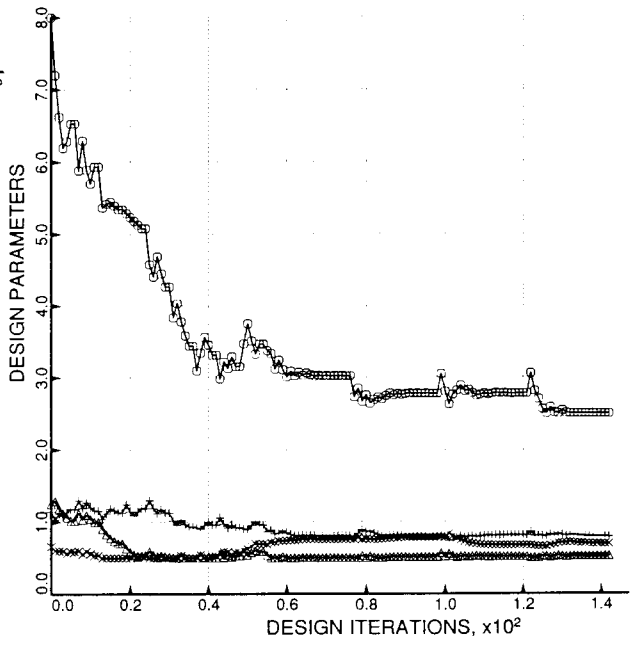


Fig. 27 Module widths; b can change

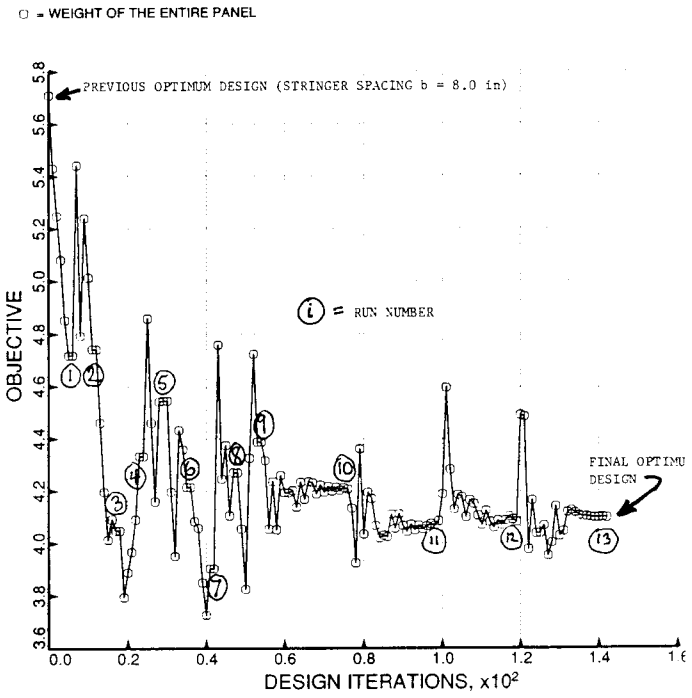


Fig. 26 Panel weight v. iterations for case with b allowed to change

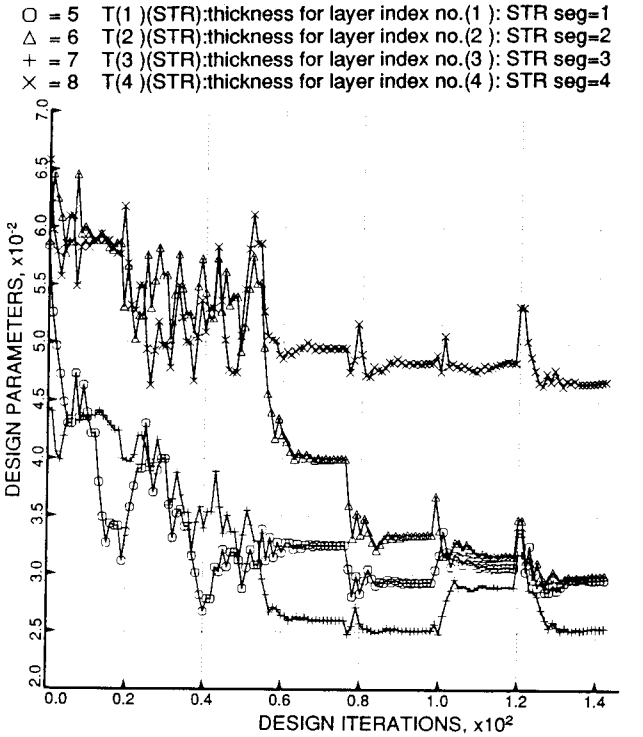


Fig. 28 Module thicknesses; b can change

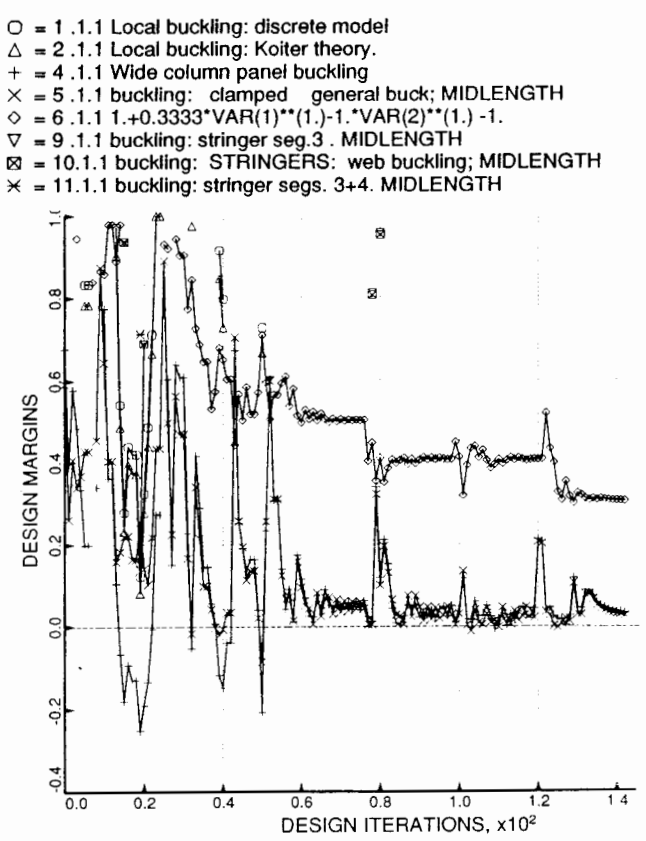


Fig. 29 Buckling margins, panel midlength, b can change

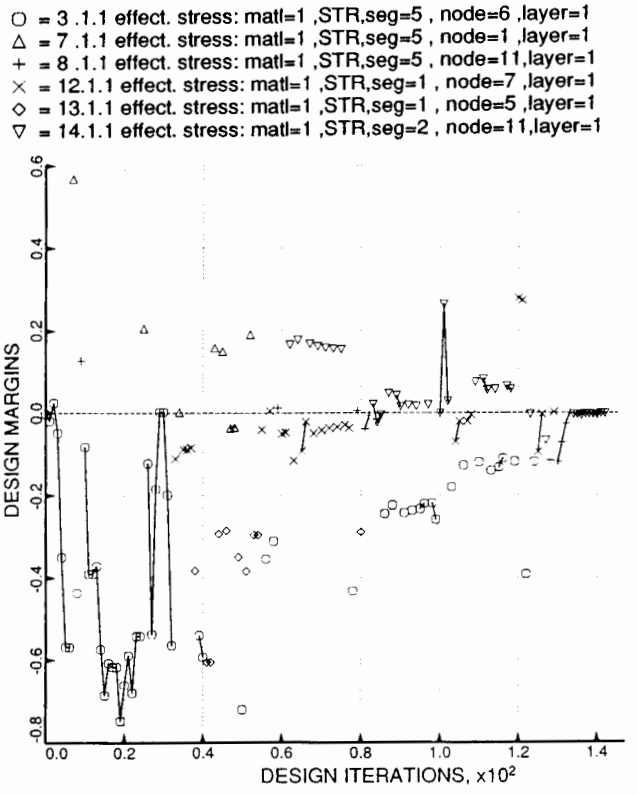


Fig. 30 Stress margins, panel midlength, b can change

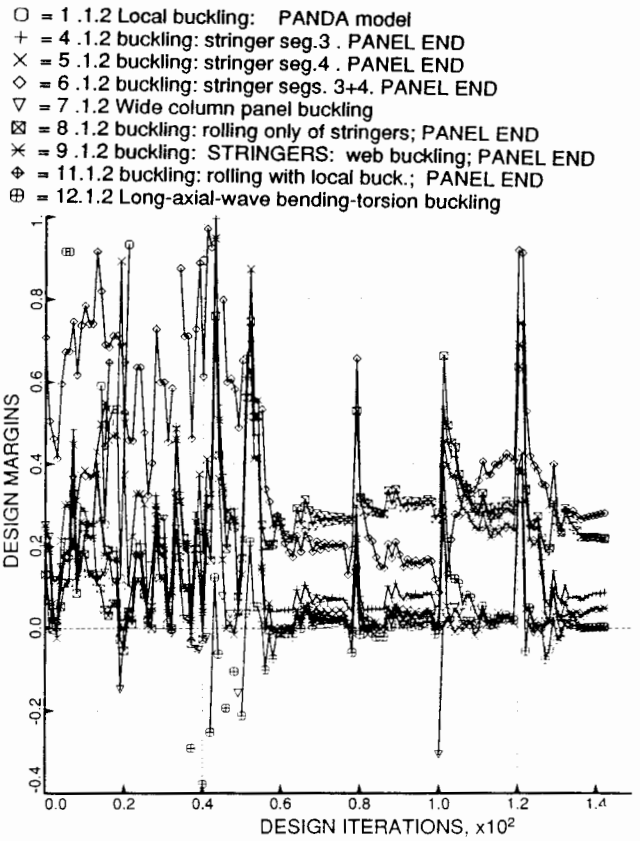


Fig. 31 Buckling margins, panel ends, b can change

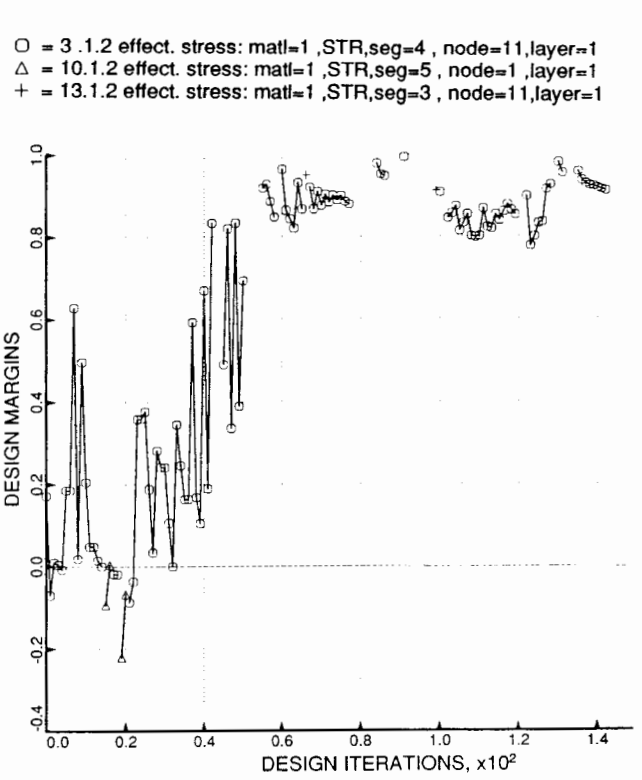


Fig. 32 Stress margins, panel ends, b can change

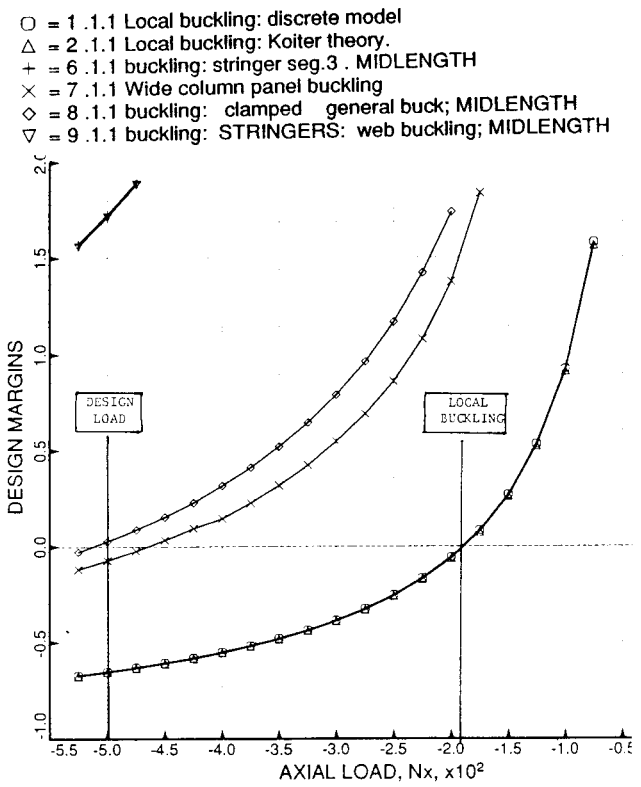


Fig. 33 Buckling margins, panel midlength, b = 2.5 in., test simulation run

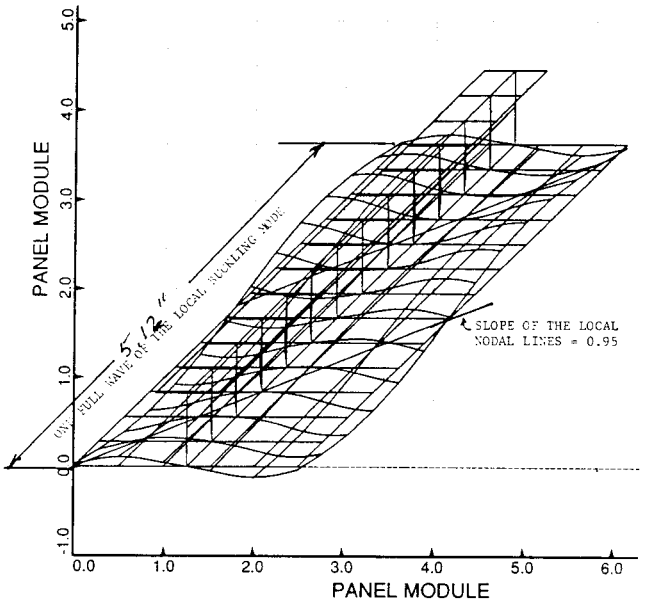


Fig. 35 Deformed module, panel midlength, b = 2.5 in., test simulation run, 3-D view

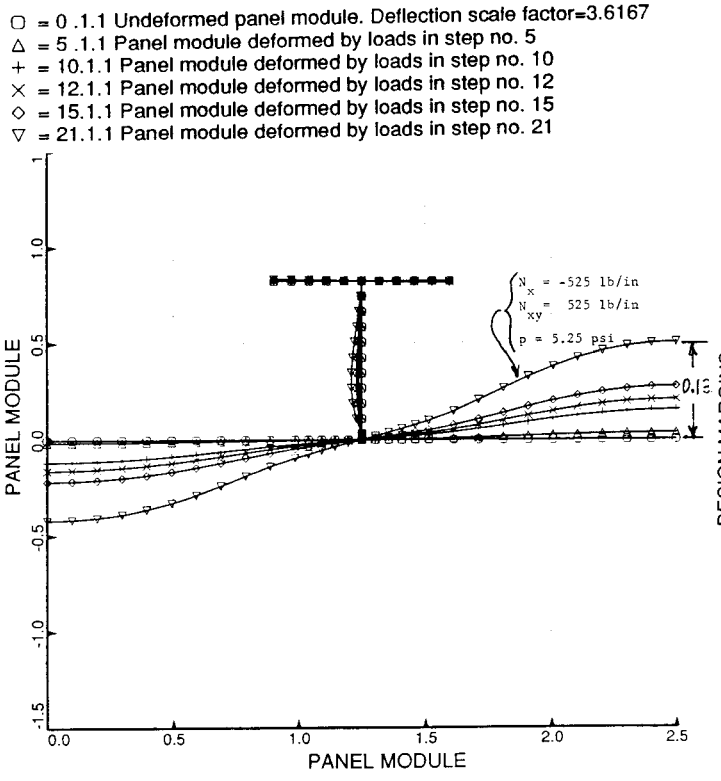


Fig. 34 Deformed module, panel midlength, b = 2.5 in., test simulation run

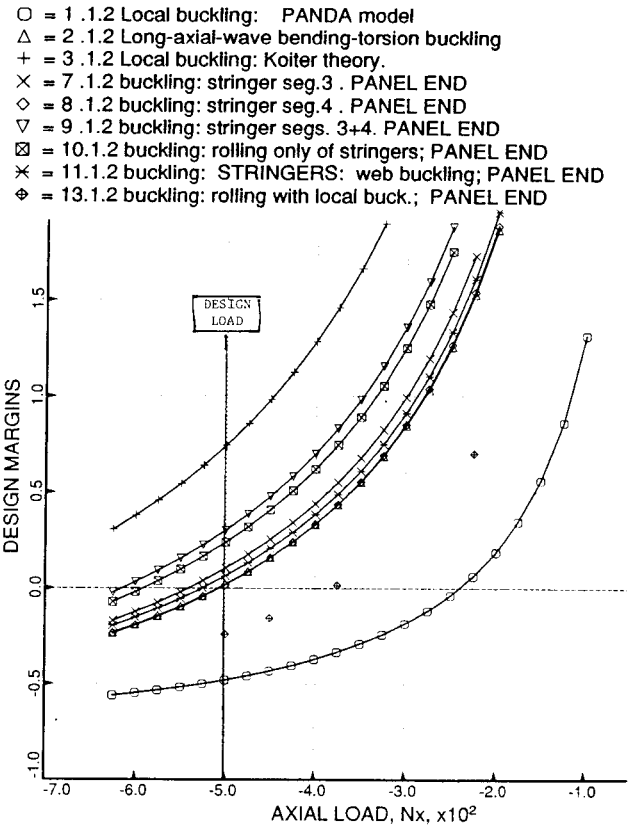


Fig. 36 Buckling margins, panel ends, b = 2.5 in., test simulation run

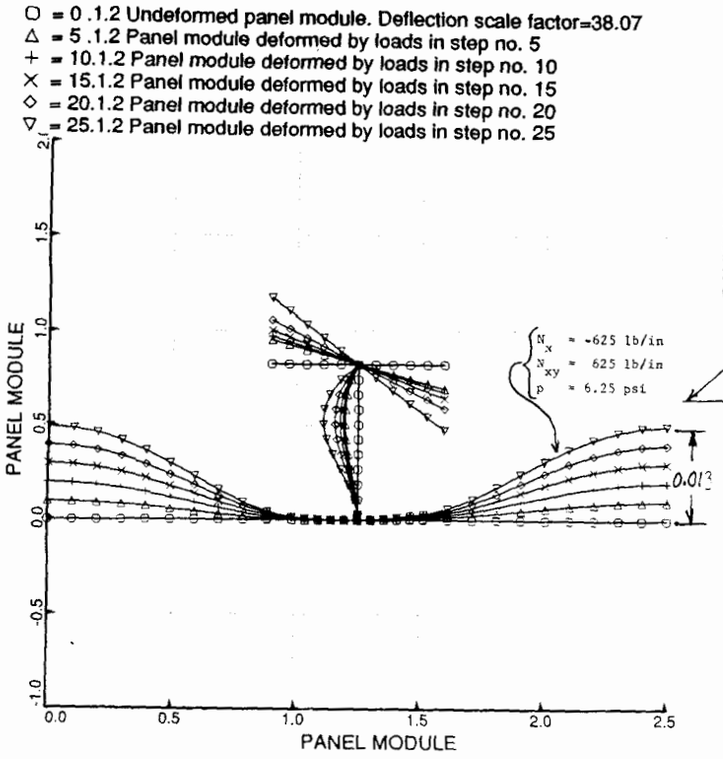


Fig. 37 Deformed module, panel ends, b = 2.5 in., test simulation run

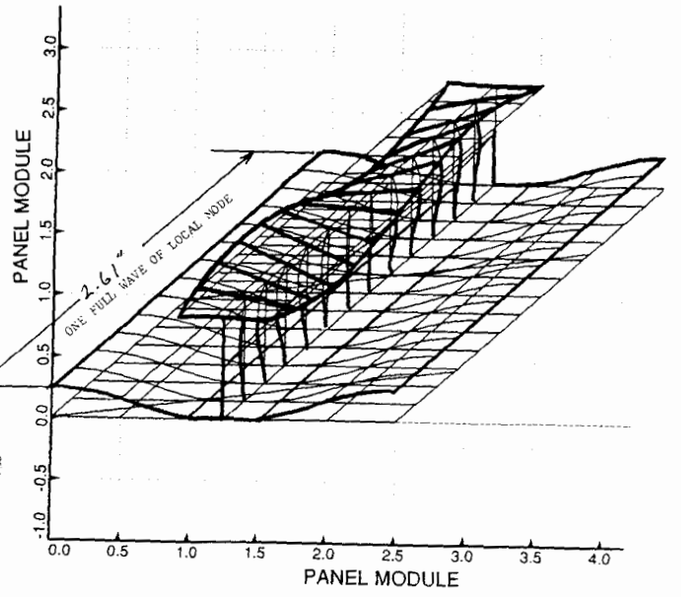


Fig. 38 Deformed module, panel ends, b = 2.5 in., test simulation run, 3-D view

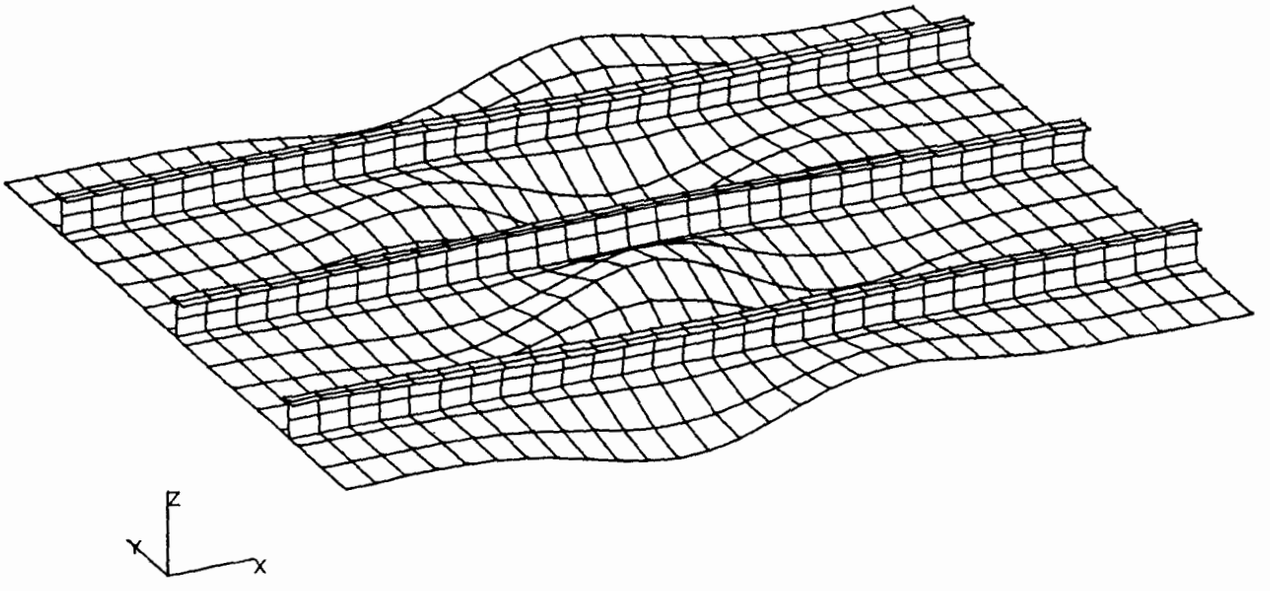


Fig. 39 Local buckling mode predicted by the STAGS computer program for a finite element model automatically generated via the new PANDA2 processor, STAGSMODEL